

EFFECT OF MANNAN-REDUCED GOLD NANOPARTICLES ON PROSTATE
CANCER CELLS



by
Nur Selin Kaya

Submitted to Graduate School of Natural and Applied Sciences
in Partial Fulfillment of the Requirements
for the Degree of Master of Science in
Biotechnology

Yeditepe University
2016

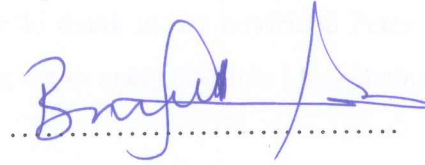
EFFECT OF MANNAN-REDUCED GOLD NANOPARTICLES ON PROSTATE
CANCER CELLS

APPROVED BY:

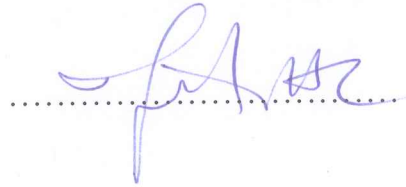
Prof. Dr. Mustafa Çulha
(Thesis Supervisor)



Prof. Dr. Bahattin Yalçın



Assist. Prof. Dr. Hüseyin Çimen



DATE OF APPROVAL: / / 2016

ACKNOWLEDGEMENTS

First, I would like to express my deepest appreciation to my supervisor, Prof. Mustafa ulha, for his guidance, continuous supports and suggestions about my proceeding experiments during my master study.

Moreover, I would like to thank to Yeditepe University Nanobiotechnology Group Members for always being there when I need something. Special thanks to Mine Altunbek, Pınar Akkuş Süt and Gamze Kuku for their technical and intellectual support throughout my scientific works. I would like to thank my labmate Gizem Uçankuş, my friend Dilara Tüzün for their moral support.

Finally, my deepest heart-felt gratitude is to my family to whom this dissertation was dedicated to. I would like to thank to my father Metin Kaya, my mother Tülay Kaya, my sisters Seray Kaya and Nurhayat Kaya for always believing and supporting me, no matter what it is. Last but not least, I would like to thank to my boyfriend Peter Horstmann for always being there for me and encouraging me in every obstacle I had encountered.

I would like to acknowledge TUBITAK for financial support during my master study.

ABSTRACT

EFFECT OF MANNAN-REDUCED GOLD NANOPARTICLES ON PROSTATE CANCER CELLS

Prostate cancer is a severe cancer type which kills a large number of males every year. The new nanotechnological therapeutic tools based on the targeting of the over-expressed receptors have showed advances to decrease the side effects on healthy cells. In this thesis, gold nanoparticles were synthesized using mannan (M-AuNPs), which is a polymer of mannose, attaches the mannose 6-phosphate receptor (M6PR) highly expressed in prostate cancer. AuNPs were used as anticancer drug delivery vehicle and their efficiency was compared with other gold nanoparticles reduced with starch and citrate on healthy PNT1A and cancerous DU145 cells. The results showed that the synthesized AuNPs did not influence the viability of the both cell lines. Dox-loaded AuNPs displayed a high rate of toxicity on DU145 cancer cells by inducing cell cycle arrest in G2/M phase. As a conclusion, M-AuNPs can be a promising tool for prostate cancer by combining with photothermal therapy.

ÖZET

MANNAN İLE İNDİRGENMİŞ ALTIN NANOPARÇACIKLARIN PROSTAT KANSER HÜCRELERİNE ETKİSİ

Prostat kanseri, her yıl ciddi sayıda erkeğin ölümüne yol açan bir kanser türüdür. Anlatımı artmış reseptörlerin hedeflenmesine dayalı yeni nanoteknolojik terapötik araçlar sağlıklı hücrelere yan etkilerin azaltılmasında önemli gelişmeler göstermiştir. Bu tezde, prostat kanserinde yüksek miktarda bulunan mannoz-6-fosfat reseptörü (M6PR) hedeflenmiş ve hedeflemede bir mannoz polimeri olan mannan ile indirgenmiş altın nanoparçacıklar (M-AuNP) kullanılmıştır. Doksorubisin anti-kanser ilacının verimliliği, sağlıklı PNT1A ve kanserli DU145 hücreleri üzerinde, ilaç dağıtım aracı olarak mannan, sitrat ve nişasta ile indirgenmiş altın parçacıklar kullanarak kıyaslanmıştır. Sonuçlarda, sentezlenen altın nanoparçacıkların her iki hücre tipinin de canlılığını etkilemediği gözlenmiştir. Dox yüklü, mannanla indirgenmiş altın nanoparçacıkların DU145 kanserli hücreleri hücre döngüsünde G2/M fazında durdurarak, canlılığı önemli oranda düşürdüğü gözlemlenmiştir. Sonuç olarak, mannan ile indirgenmiş altın nanoparçacıkların fototermal terapi ile birleştirilerek prostat kanserinin tedavisinde gelecek vaad eden bir araç olabileceği düşünülmektedir.

TABLE OF CONTENTS

ACKNOWLEDGEMENTS	iii
ABSTRACT.....	iv
ÖZET	v
LIST OF FIGURES	viii
LIST OF TABLES	x
LIST OF SYMBOLS/ABBREVIATIONS.....	xi
1. INTRODUCTION	1
1.1. GOLD NANOPARTICLES.....	3
1.1.1. AuNP Synthesis Methods	4
1.1.2. Advantages of AuNPs in Biomedical Applications.....	5
1.2. AuNPs in DRUG DELIVERY	8
1.2.1. Passive Targeting Strategies	8
1.2.2. Active Targeting Strategies	8
1.2.3. Doxorubicin	9
1.3. MANNAN	9
1.3.1. Mannan-based Drug Targeting Systems.....	10
1.4. AIM OF THE STUDY	11
2. MATERIALS AND METHODS.....	12
2.1. SYNTHESIS OF GOLD NANOPARTICLES	12
2.1.1. Synthesis of Mannan Reduced Gold Nanoparticles (M-AuNPs)	12
2.1.2. Synthesis of Citrate Reduced Gold Nanoparticles (C-AuNPs)	12
2.1.3. Synthesis of Starch Reduced Gold Nanoparticles (S-AuNPs).....	12
2.1.4. Doxorubicin Conjugation of Gold Nanoparticles	13
2.2. CHARACTERIZATION OF SYNTHESIZED GOLD NANOPARTICLES	13
2.2.1. UV/Vis Absorption Spectroscopy	13
2.2.2. Dynamic Light Scattering (Zeta Sizer).....	13
2.3. CELL CULTURE	13
2.3.1. WST-1 Cell Viability Assay	14
2.3.2. Cell Cycle Assay.....	14
2.3.3. Intracellular Uptake of M-AuNP	14
3. RESULTS	16

3.1. CHARACTERIZATION OF AUNPs.....	16
3.2. WST-1 CELL VIABILITY ASSAY.....	23
3.3. CELL CYCLE ANALYSIS.....	27
3.4. INTRACELLULAR ACCUMULATION OF M-AUNPs.....	28
4. DISCUSSION.....	29
5. CONCLUSIONS.....	32
REFERENCES.....	33



LIST OF FIGURES

Figure 1.1. Major properties of gold nanoparticles	3
Figure 1.2. Applications of gold nanoparticles for cancer therapy	5
Figure 1.3. Two different type of functionalization of gold nanoparticles mainly used in delivery applications	7
Figure 1.4. Preparation of Doxorubicin conjugated AuNPs	9
Figure 1.5. Structure of mannan polysaccharide.....	9
Figure 3.1. UV/Vis spectra of M-AuNPs, C-AuNPs and S-AuNPs.	17
Figure 3.2. Size distribution of mannan-reduced AuNP and Dox-loaded AuNPs in DLS Analysis.	18
Figure 3.3. AFM image of M-AuNPs.....	19
Figure 3.4. Image of M-AuNPs, C-AuNPs, S-AuNPs and their Dox loaded forms.....	20
Figure 3.5. Comparison of absorption spectra of bare M-AuNPs and Dox-conjugated M-AuNPs.....	21
Figure 3.6. Comparison of absorption spectra of S-AuNP and Dox-conjugated S-AuNPs.....	21
Figure 3.7. Reproducibility of AuNPs conjugation with Doxorubicin.....	22
Figure 3.8. DLS spectra of bare and Dox-loaded M-AuNPs.....	23

Figure 3.9. DLS spectra of bare and Dox-loaded S-AuNPs.	23
Figure 3.10. Cell viability of (A) PNT1A and (B) DU145 cells after exposure of M-AuNPs, mannan, M-AuNP-Dox and free Dox for 24 h.....	25
Figure 3.11. Cell viability of (A) PNT1A and (B) DU145 cells after exposure of M-AuNPs and C-AuNPs.....	26
Figure 3.12. Cell viability of (A) PNT1A and (B) DU145 cells after exposure of S-AuNPs, Dox, and S-AuNP-Dox conjugates.....	27

LIST OF TABLES

Table 3.1. Cell cycle results of PNT1A normal prostate cell line.	28
Table 3.2. Cell cycle results of DU145 carcinoma prostate cell line.....	29
Table 3.3. Amount of Au accumulated inside cells after ICP-MS.....	30



LIST OF SYMBOLS/ABBREVIATIONS

Au	Gold
AuNP	Gold Nanoparticle
C-AuNP	Citrate-reduced Gold Nanoparticles
CT	Computed Tomography
Dox	Doxorubicin
DU145	Human prostate carcinoma cell line
EPR	Enhanced Permeation and Retention
ER	Enhanced Retention
M-AuNP	Mannan-reduced Gold Nanoparticles
MPS	Mononuclear Phagocyte System
NP	Nanoparticle
PNT1A	Human prostat normal cell line
S-AuNP	Starch-reduced Gold Nanoparticles

1. INTRODUCTION

There are various research and development about nanoparticle-based diagnostics and therapeutics so far [3]. The remarkable potential of NPs in gene therapy, targeted drug delivery, imaging, stem cell tracking and differentiation, immunotherapy, photo-ablation therapy has been observed [4-8]. Many different nanocarriers such as polymer micelles and vesicles, nanocapsules, dendrimers, metal NPs and liposomes have been used in delivery system [9-13]. Gold nanoparticles (AuNPs) have recently emerged as an attractive structures due to their applications in biology, optics, catalysis and chemical sensing [14]. The reason of popularity of AuNPs comes from that can be applied for cancer targeted drug delivery as well as imaging. The physicochemical properties of AuNPs which separate them from other nanoplatforms are mainly suitable optical properties for being used as imaging agents, chemical inertness, easy surface functionalizability and conformable electronic structure for Plasmon resonance [15]. Another important feature of AuNPs is due to their widely ranged core sizes from 1 to 150 nm can be synthesized not only easily but also with controlled dispersity. Size and dispersity are important issues for drug delivery systems [16].

Prostate cancer is one of the most death causing type of cancer in males. In 2010, the total medical costs for prostate cancer was 12 billion [25]. Around 220,000 men diagnosed with this type of cancer and around 27,000 of them died from this disease in USA in 2014 [26]. Prostatectomy, radiotherapy or brachytherapy are mainly applied to patients in early stages [27]. However, these methods have drawbacks. Prostatectomy is the removal of prostate glands from patients and patients whom applied prostatectomy become infertile after surgery. Radiotherapy is a non-selective method which also affects the whole body. Brachytherapy is an advanced method for early-stage of prostate cancer. Radioactive seeds are placed in tumor area and cells are treated by high radiation. This is a localized, précised and high-tech technique. However, it uses radiotherapy as treatment method so it might cause side effects in that localized area as well. For advanced stages, androgen deprivation therapy (ADT), which targets androgen receptor in a specific localization, is performed as a standard procedure. Prostate cancer cells need androgen hormones and by this technique, androgen hormones are reduced in cancer cells and growth is slowed down. Since ADT only makes the growth slower, radiation therapy should be applied after ADT. Due to the

side effects of radiation, this therapy is also not the most efficient way to treat prostate cancer[28]. This is why new, non-toxic and more efficient drug delivery systems have been investigated in the last few decades.

Chemotherapy is one of the main auxiliary therapeutic options for the treatment of metastatic cancer. However, it has a crucial problem about the chemotherapeutic agents because they cannot differentiate normal and cancerous cells. This causes consequential damage on normal cells as well. One of the problems on the basis of this inefficiency is resulted from that interstitial fluid pressure in solid tumor is more than in normal tissue and this reduces the transcapillary transportation of chemotherapeutic agents into the target tumor areas [29-30]. Furthermore, due to the damaging side effects of chemotherapeutic agents, insufficient amount is treated to the patients, which lead to incomplete response from tumor and thus, drug resistance by time [31].

Different nanocarrier systems for drug delivery were developed for treatment of prostate cancer. By synthesizing NP-drug conjugations, it was aimed to improve solubility, bioavailability, biocompatibility, retention time and pharmacokinetics behavior [91]. NPs were modified with hyaluronic acid and conjugated with cisplatin to reduce side effects of chemotherapeutic drug for targeted delivery of prostate cancer cells by using CD44 surface marker [92]. In another study, catechin attached-carbon nanotubes were explored as a possible nanocarrier system for targeting prostate cells [93]. In combination with X-ray irradiation, catechin-loaded gelatin NPs and carbon nanotubes showed promising results for treatment of prostate cancer [94]. Kulhari *et al.* showed that succinoyl TPGS nanomicelles conjugated with cyclic peptide (cRGDfK) can be used efficiently for targeted drug delivery of docetaxel in prostate cancerous cells [95]. Magnetic iron NPs are also used widely for diagnostic and theranostic applications. Magnetic iron nanoparticles were conjugated with Dox, *in vitro* and *in vivo* studies indicated that they NP-Dox clusters induces high toxicity for PC3 prostate cancer cells. by light-triggered Dox release and photo-ablation [96]. Axiak-Bechtel *et al.* studied the cytotoxic effect of gum-Arabic coated radioactive gold NPs in prostate cells and it caused minimal short-term toxicity [97]. In the study of Vaillant *et al.*, mesoporous silica NPs were functionalized with analogue of mannose-6-phosphate receptor. It was proven that these NPs can be used for targeted drug delivery in prostate cancer cells using photodynamic therapy [67].

1.1. GOLD NANOPARTICLES

Nanotechnology can be described as controlling the size and shape at nanometer scale in design, production, characterization and application of structures, devices and systems [1]. Nanoparticles (NPs) get attention due to their desirable physicochemical properties [2]. Many different nanocarriers such as polymer micelles and vesicles, nanocapsules, dendrimers, metal nanoparticles and liposomes have been used as delivery system [9-13]. AuNPs have recently emerged as an attractive structure due to their applications in biology, optics, catalysis and chemical sensing [14]. Figure 1.1. shows the schematic representation for the AuNPs properties.

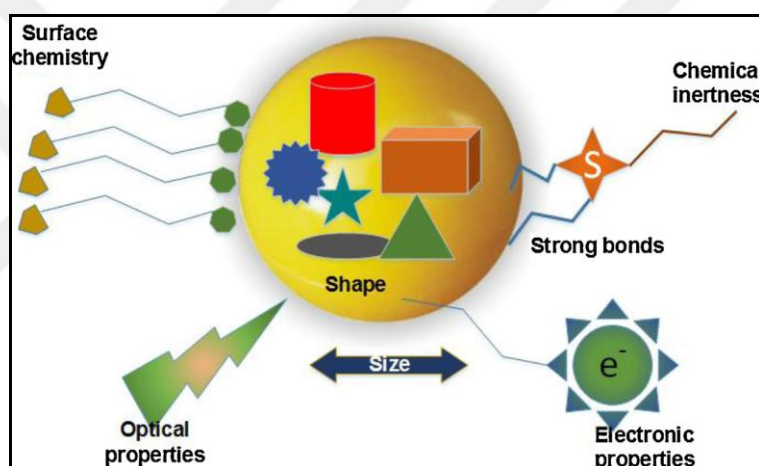


Figure 1.1. Major properties of gold nanoparticles [8].

AuNPs interact with the light in the visible region, absorb strongly and scatter it more than other nanomaterials [52]. When the light is absorbed, it starts the oscillation of the conduction band electrons of metal. The electron oscillation around the surface of nanoparticle induces formation of dipole oscillation along the direction of electric field of incident light. When the amplitude of the oscillation is in maximum at a specific frequency, this is called as Surface Plasmon Resonance (SPR) [17]. SPR band is much stronger in AuNPs comparing to other metal NPs. AuNPs show a strong SPR band in visible region [52]. SPR frequency is dependent on size, shape, surface properties of nanoparticle, interactions between nanoparticles and dielectric properties of surrounding medium [18]. Any difference in one of those parameters can be differentiated with optical

resonance using UV/Vis Absorption Spectroscopy by showing a shift in absorption wavelength [19].

1.1.1. AuNP Synthesis Methods

AuNPs can be easily synthesized with controlled dispersity in a range of 1 to 150 nm using bottom-up and top-down methods [73]. Nanosphere lithography, chemical, electrochemical, photochemical, sonochemical, templating and thermal reduction techniques are based on bottom-up method [74-76]. This method is applied by the reduction of ions producing desired nanostructures. Au salts are reduced in the presence of surface stabilizers, which inhibit the aggregation of Au in the solution by attractive Van der Waals and depletion forces [72]. Top-down methods, which are photolithography and electron beam lithography, are performed by that the matter is removed from the bulk material for production of nanoparticles [77-78]. There are 5 commonly used techniques for synthesis of AuNPs: Turkevich, Brust, seeded growth, digestive ripening and miscellaneous methods. Turkevich method is the most common way of synthesizing spherical AuNPs. Gold ions (Au^{+3}) are reduced to Au^0 atoms by citrate, ascorbic acid, aminoacids or UV light [79-80]. In Brust method, firstly gold salt is transferred to an organic solvent from aqueous solution and then, reduced by sodium borohydride [81]. Turkevich and Brust methods are used generally for synthesis of spherical gold nanoparticles. When other shapes of gold nanoparticles are desired, seeded growth method is used. In this method, gold salt is reduced with sodium borohydride to obtain seed particles, then the solution is transferred to metal salt solution with a weaker reducing agent such as ascorbic acid. By changing the concentrations of seeds, shape of gold nanoparticles can be altered [82]. In digestive ripening technique, gold nanoparticles are synthesized using excessive ligands in the presence of alkanethiols. Thiols, amines or silanes can be used as ligand in this method. The most important issue is the high temperature in this type of synthesis for control of size distribution of AuNPs [83]. Miscellaneous methods include ultrasonic waves, microwaves, laser ablation, solvothermal method, electrochemical and photothermal reduction techniques which are used for synthesis of AuNPs [80].

Methods explained above are used widely for production of AuNPs. However, they have a drawback of generating toxic byproducts that can induce toxicity, which is an important issue for drug delivery systems [16]. To overcome this problem, new strategies were developed with non-toxic chemicals. These strategies are based on the principles of green chemistry which uses biodegradable reagents by reducing waste products and toxicity, and provides production at desired temperature and pressure [84].

1.1.2. Advantages of AuNPs in Biomedical Applications

The AuNPs can be applied for cancer targeted drug delivery as well as imaging due to the physicochemical properties of AuNPs which separate them from other nanoplatforms with suitable optical properties, chemical inertness, easy surface functionalizability and conformable electronic structure for surface Plasmon resonance (SPR) [15]. Figure 1.2 shows the application fields of AuNPs in theranostics [8].

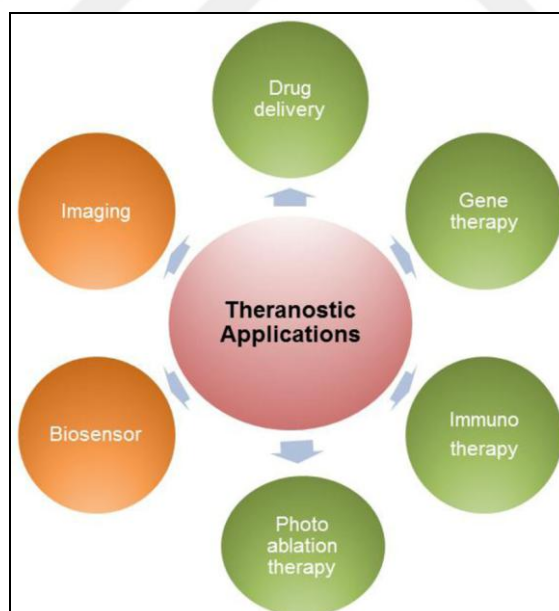


Figure 1.2. Applications of gold nanoparticles for cancer therapy [8].

The particle size is a major key for circulation and biodistribution of nanoparticles. While NPs smaller than 10 nm are cleared quickly from the body by the kidneys or through extravasation, larger NPs can be caught by mononuclear phagocyte system (MPS) [40]. As a result of many studies, nanoparticles smaller than 100 nm have a longer circulation time in blood and exposed to reduced hepatic filtration. Size of nanoparticles also affects the accumulation in tumor site via EPR [41]. The optimum size range for nanoparticles to escape from physiological barriers and take advantage on EPR effect should be 10-250 nm [42]. Surface charge of NPs can cause them to be caught by MPS. Neutrally charged NPs have less opsonization rates compared to charged nanoparticles[43-44]. Positively charged NPs induces higher phagocytic uptake than neutrally or negatively charged NPs [45]. Davis et al. proposed that NP surface charge should be in the range of -10 and +10 mV to reduce phagocytosis and nonspecific interactions of NPs [46].

AuNPs have a high surface area to volume ratio which increases the loading amount of functionalities onto the nanoparticle surface [20]. They also provide diversity about the conjugation of different therapeutic drugs or biomacromolecules onto the nanoparticle surface covalently or non-covalently, due to their multivalent and tunable surface characteristics [21-22].]. Figure 1.3. shows the two different type of functionalization of gold nanoparticles mainly used in delivery applications.

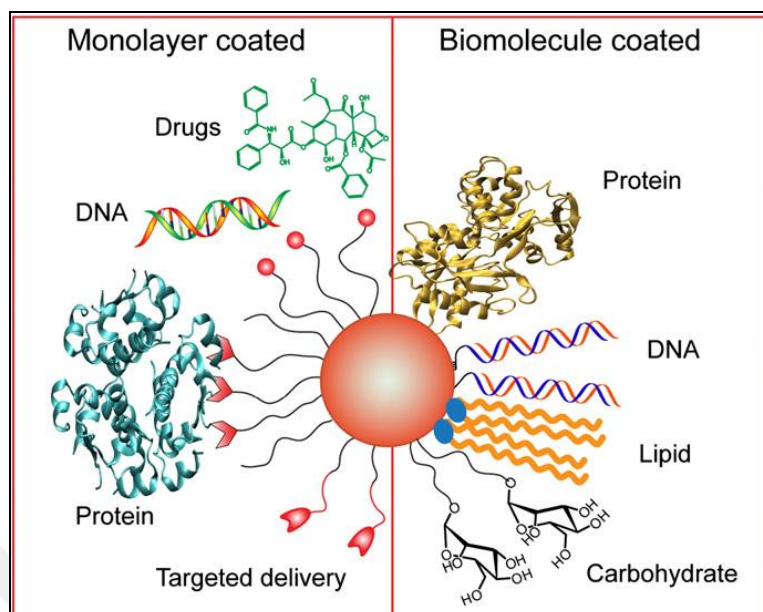


Figure 1.3. Two different type of functionalization of gold nanoparticles mainly used in delivery applications [24].

AuNPs display strong optical absorbance in the NIR tissue optical transparency range. An energy source such as laser generates nonionising electromagnetic radiation when it is applied to a specific area. With the applied energy to gold nanoparticles, energy is converted to heat by electron excitation and relaxation on the surface of AuNPs. With the heat release from AuNPs, temperature rises in that local area and this phenomenon is called as hyperthermia. Hyperthermia is one of the possible treatment methods for cancer. It causes apoptotic cell death and increases local control. This method can be used also in combination with radiotherapy and chemotherapy [53-55]. It can be applied with heat generation by radiofrequency waves, ultrasound or microwaves [56]. Due to side effects of chemotherapeutic agents, photothermal therapy is combined with chemotherapy to use lower dose of chemotherapeutic agents and increase the effect with hyperthermia. Toxic heat and drugs work simultaneously and locally on tumor sites. In chemo-photothermal therapy, cancer cells are not only affected by the cytotoxicity of drugs but also sensitized by high temperatures on targeted area [57-61].

1.2. AuNPs in DRUG DELIVERY

Due to toxic side effects of anti-cancer drugs, new, non-toxic and more efficient drug delivery systems has been investigated in the last few decades. Nanocarriers are found out as useful tool as drug delivery systems in numerous studies [32].

Drugs can be loaded onto nanoparticle surface covalently or non-covalently. When the conjugation is covalent, the nanocarrier platform is formed more stable. Nevertheless, the prodrug should be processed intracellularly [33]. In non-covalent conjugation of drugs with nanoparticles, active drug is released in cells directly, but the disadvantage of this method is the possibility of premature release [24].

1.2.1. Passive Targeting Strategies

Gold nanoparticles can penetrate into tumor tissue via enhanced permeation and retention (EPR) effect through the leaky vasculatures in tumor site. Since vasculatures in tumor site are super-leaky, AuNPs can reach to the interstitial space of the tumor by EPR effect. Moreover, clearance of gold nanoparticles from tumor site is limited by impaired lymphatic drainage, thereby this induces enhanced retention (ER) of nanoparticles. These two cases occur because of the fast growth of tumor tissue and the collapse of blood and lymph vessels in that area [34].

1.2.2. Active Targeting Strategies

For active targeting of gold nanoparticles, ligands such as peptides, proteins, nucleic acids or antibodies with high affinity to a specific receptor which are over-expressed in tumor tissue are conjugated to nanoparticles. Due to multivalent surface characteristics of gold nanoparticles, the surface of nanoparticles can be loaded with different type of ligands to increase the efficiency of cellular uptake and enhance the targeting [8].

1.2.3. Doxorubicin

Doxorubicin is an anti-cancer drug used for the treatment of many different cancer types. The anti-tumor activity is performed by intercalating DNA. It interacts with DNA replicative system in the cell nucleus [35].

Doxorubicin conjugated gold nanoparticles can enhance computed tomography (CT) imaging contrast and used for photothermal cancer therapy [37]. Doxorubicin can be conjugated to gold nanoparticles in two ways. Firstly, a linker molecule can be utilized for covalent conjugation [37-39]. Secondly, the conjugation can be achieved by electrostatic interactions or hydrogen bonds. Second method can be advantageous because linker molecule is unnecessary and drug release into the cells would be easier than in covalent conjugation [36]. The electrostatic interactions between Dox and gold nanoparticles are illustrated in Figure 1.4.

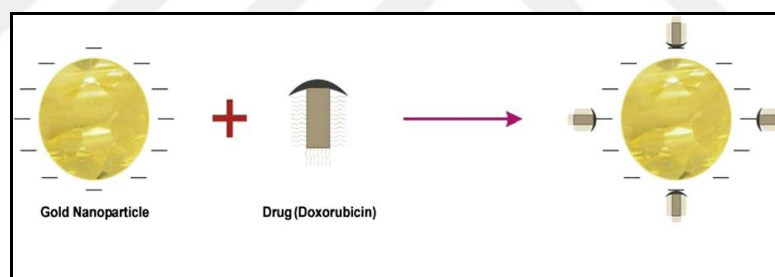


Figure 1.4. Preparation of Doxorubicin conjugated AuNPs [36].

1.3. MANNAN

Mannan is a polymer of mannose sugar. Mannan can be found in 4 different forms in nature which are linear mannan, glucomannan, galactomannan and galactoglucomannan. Each type is named according to the composition of sugar monomers in the polymer. A linear mannan contains mannose residues in a linear arrangement with β -1,4-linked

backbone. All types of mannans have this backbone [47-49]. Structure of mannan is shown in Figure 1.5.

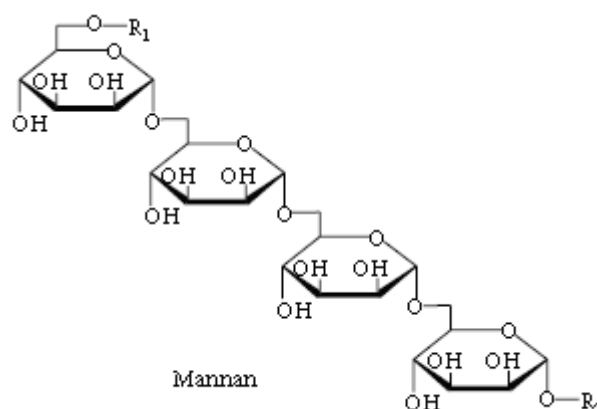


Figure 1.5. Structure of mannan polysaccharide.

Mammalian cells are covered with high density of carbohydrates on the surface. Cell surface carbohydrates have crucial role in cell-cell recognition, inflammation, metastasis, infection, immune surveillance of tumors and cancer [63-65]. AuNPs conjugated with carbohydrates increases the biocompatibility, targeting ability and maintains higher delivery efficiency [24].

1.3.1. Mannan-based Drug Targeting Systems

Mannan, which is recognized by the mannose receptors easily on the surface of antigen-presenting cells, has a distinctive property than other polysaccharides. This makes the uptake of mannan-bearing nanoparticles into the cells easier via mannose-mediated endocytosis and phagocytosis. [62]

The use of mannan has been reported in drug delivery systems. In study of Apostolopoulos *et al.*, mannan was oxidized and conjugated with MUC1 fusion protein. This drug delivery system was used for tumor immunotherapy in treatment of early-stage of breast cancer [85]. Ferreira *et al.*, prepared nanogel from mannan and cytocompatibility was investigated

in mouse embryo fibroblast (3T3) and mouse-macrophage-like (J774) cells. It was shown that mannose residues were bound to mannose-binding receptors on cell surface and these complexes were internalized through the endocytic pathway. It was confirmed that mannan nanogels have high toxicity in macrophage-like cells but primary cultures of macrophages are more suitable for the application of mannan nanogels [86]. In 2012, he and his team studied the mannan nanogel cytocompatibility on mouse embryo fibroblast (3T3) and mouse bone marrow-derived macrophage (BMDM) cells. It was indicated that mannan nanogel induces DNA damage on mouse BMDM but no cytotoxicity in 3T3 cells [87].

Moreover, superparamagnetic iron oxide nanoparticles (SPIONs) were coated with mannan and used for targeted delivery to macrophages. Vu-Quang *et al.* investigated the physicochemical properties of carboxylic mannan-coated SPIONs (CM-SPIONs) using MRI. It was demonstrated that CM-SPIONs stay longer in blood circulation than M-SPIONs and claimed that CM-SPIONs can be potential contrast agent for MRI [88].

Konjac glucomannan (KGM) is a water soluble polysaccharide. It was shown that KGM is degraded by colon β -mannanase which is secreted from human colon bacteria. KGM is a stable and non-cytotoxic material for drug delivery [89].

Kaur *et al.* investigated mannan-coated gelatin nanoparticles for targeted delivery of didanosine for HIV. Mannan-coated nanoparticles were uptaken more by macrophage cells and drug release was retarded. It was concluded that due to mannose-binding receptors on cell surface of macrophages, mannan-coated NPs are penetrating into cells more [90].

1.4. AIM OF THE STUDY

AuNPs due to their many advantageous properties have been used for many drug delivery systems for various diseases. Due to high abundance of mannose binding lectins on the surface of prostate cancer cells, mannan reduced AuNPs can be an efficient tool for treatment of prostate cancer. In this study, it was aimed to investigate the effect of doxorubicin conjugated mannan-reduced AuNPs on DU145 prostate cancer cell line, examine the cytotoxicity of these nanocarriers on both normal and malignant (PNT1A and DU145, respectively) prostate cancer cells and compare mannan-reduced AuNPs to citrate and starch-reduced AuNPs.

2. MATERIALS AND METHODS

2.1. SYNTHESIS OF GOLD NANOPARTICLES

2.1.1. Synthesis of Mannan Reduced Gold Nanoparticles (M-AuNPs)

The AuNPs were synthesized by mannan reduction of $\text{HAuCl}_4 \cdot 3\text{H}_2\text{O}$ (#27988-77-8, Sigma, Germany) with sodium hydroxide (NaOH, #67-56-1, Sigma-Aldrich, USA) [50]. 5 mL of 10 mM $\text{HAuCl}_4 \cdot 3\text{H}_2\text{O}$ was mixed with 5 mL of 0.04 M NaOH solution and incubated for 15 min. A 25 mg of mannan (#9036-88-8, Sigma-Aldrich, USA) was dissolved in 5 mL of dH_2O and mixed with 5 mL of 0.02 M NaOH solution. The mixture was heated to 80°C and incubated for 15 min. The mannan and prepared gold solutions were mixed and stirred at 80°C for 30 min. The gold colloid was cooled down to room temperature and the final volume of the colloid was adjusted to 20 mL with dH_2O .

2.1.2. Synthesis of Citrate Reduced Gold Nanoparticles (C-AuNPs)

The AuNPs were synthesized by sodium citrate reduction of $\text{HAuCl}_4 \cdot 3\text{H}_2\text{O}$ [51]. 100 mL of 1mM $\text{HAuCl}_4 \cdot 3\text{H}_2\text{O}$ solution was heated until boiling. After the solution is boiled, 10 mL of citrate stock solution (38.8 mM of trisodium citrate (#6132-04-3, Sigma-Aldrich, USA) dissolved in 10 mL of water) was mixed with boiling gold solution, rapidly. Then, the color of the solution changes from yellow to black and finally to dark red. The final solution was kept boiling for 15 min.

2.1.3. Synthesis of Starch Reduced Gold Nanoparticles (S-AuNPs)

The AuNPs were synthesized by starch reduction of $\text{HAuCl}_4 \cdot 3\text{H}_2\text{O}$ (#27988-77-8, Sigma, Germany) in the alkaline condition using the similar procedure used for mannan reduction [50]. Briefly, a 5 mL of 10 mM $\text{HAuCl}_4 \cdot 3\text{H}_2\text{O}$ was mixed with 5 mL of 0.04 M NaOH solution and incubated for 15 min. A 100 mg starch dissolved in 5 mL of dH_2O (#9005-84-9, Sigma-Aldrich, USA) was mixed with 5 mL of 0.02 M NaOH solution and heated to

80°C for 15 min. Then, starch-NaOH solution was mixed with Gold-NaOH solution and incubated at 80°C for 30 min. The gold colloid was cooled down to room temperature and the final volume of the colloid was adjusted to 20 mL dH₂O.

2.1.4. Doxorubicin Conjugation of Gold Nanoparticles

A 5 μ L of 1 mM Dox solution was added to 1 mL of M-AuNPs, C-AuNPs and S-AuNPs and incubated for 24h while shaking at room temperature.

2.2. CHARACTERIZATION OF SYNTHESIZED GOLD NANOPARTICLES

2.2.1. UV/Vis Absorption Spectroscopy

The plasmon absorption spectra of synthesized M-AuNPs, C-AuNPs and S-AuNPs were characterized using UV-Vis Spectrophotometer Lambda 35 (Pelkin Elmer). The changes in the absorption spectra of M-AuNPs, C-AuNPs and S-AuNPs after conjugation with Doxorubicin were also monitored with UV-Vis spectrophotometer.

2.2.2. Dynamic Light Scattering (Zeta Sizer)

The measurements were done using Malvern Zetasizer Nano ZS at 25°C at 173° scattering angle with a 4 mV He-Ne laser for both synthesized M-AuNPs, C-AuNPs and S-AuNPs and Dox-conjugated M-AuNPs, C-AuNPs and S-AuNPs. Standard disposable polystyrene cuvettes for size measurements were used. The refractive index and absorption of colloids were set as 2.0 and 0.320, respectively.

2.3. CELL CULTURE

Normal human prostate cell line (PNT1A, #95012614, Sigma-Aldrich) and human prostatic carcinoma cell line (DU145, HTB-81, ATCC) were used to monitor the efficiency of M-AuNPs, C-AuNPs and S-AuNPs for drug delivery. The cells were cultured in Dulbecco's modified Eagle's medium (DMEM, #D5546, Sigma-Aldrich) containing 10%

Fetal Bovine Serum Albumin (FBS, #3020-20, ATCC), 100 units/mL penicillin and 100 mg/mL Streptomycin (Gibco, UK), 2 mM L-glutamine (#56-85-9, Sigma-Aldrich) and were cultured at 5% CO₂ supplied at 37°C in incubator.

2.3.1. WST-1 Cell Viability Assay

PNT1A and DU145 cells were seeded on 96-well culture plate at 5000 cells/well and incubated for 24 h for cell attachment at 37°C humidified incubator supplied with 5% CO₂. Then, the medium was changed with fresh medium containing bare and Dox-conjugated conjugated M-AuNPs, C-AuNPs and S-AuNPs. The un-treated cells were used as control.

2.3.2. Cell Cycle Assay

The effect of M-AuNPs and Dox conjugated M-AuNPs on cell cycle was evaluated by comparison with free Dox treatment. Briefly, PNT1A and DU145 cells were seeded on 6-well culture plate at 150000 cells/well and incubated for 24 h for cell attachment. Then, the cells were treated with 3 nM AuNPs (mannan), 0.5 μM Dox-conjugated to AuNPs (mannan) in 3 nM concentration, 0.5 μM Dox and 0.5 μM Colchicine for 24h. Cells were removed with Trypsin and solved in PBS. After medium was removed from cells completely by centrifugation, cells were fixated in 700 μL of cold 100% ethanol and 300 μL of cold PBS. The cells were kept at +4°C during cell fixation. Then, cells were incubated at -20°C for overnight. The cells were centrifuged at 3500 rpm for 10 min and rinsed off until ethanol is removed from cells completely. Cells were solved in 400 μL of cold PBS. First, RNase A and 10 min later PI was added to cells in the ratio of 2:1. It was incubated in darkness for 15 min at ice box. The cell cycle results were acquired by EasyCyte Flow Cytometer device (GUAVA).

2.3.3. Intracellular Uptake of M-AuNP

In order to demonstrate the efficient uptake of M-AuNPs by prostate cancer cells, the M-AuNPs treated PNT1A and DU145 were examined on ICP-MS. Briefly, 30000 cells were cultured in 24-well plate for both cell lines and incubated for 24h. The un-treated cells

were used as control. After 24h incubation with 1 nM M-AuNPs, cells were washed with medium for 3 times and then rinsed with nitric acid twice and collected. After cells were sonicated, samples were filtered with 0.22 μ M filter. The final concentration was completed to 10 mL and then, ICP-MS measurement was conducted.



3. RESULTS

3.1. CHARACTERIZATION OF AUNPs

The surface plasmon absorption profile of AuNPs alters depending on size, shape, surface chemistry, agglomeration and the dispersion media. The distinctive SPR absorption profiles of mannan reduced (M-AuNPs), citrate reduced (C-AuNPs) and starch reduced (S-AuNPs) are shown in Figure 3.1. M-AuNPs have maximum absorption at 520 nm while C-AuNPs and S-AuNPs have their absorption band at 519 nm and 526 nm.

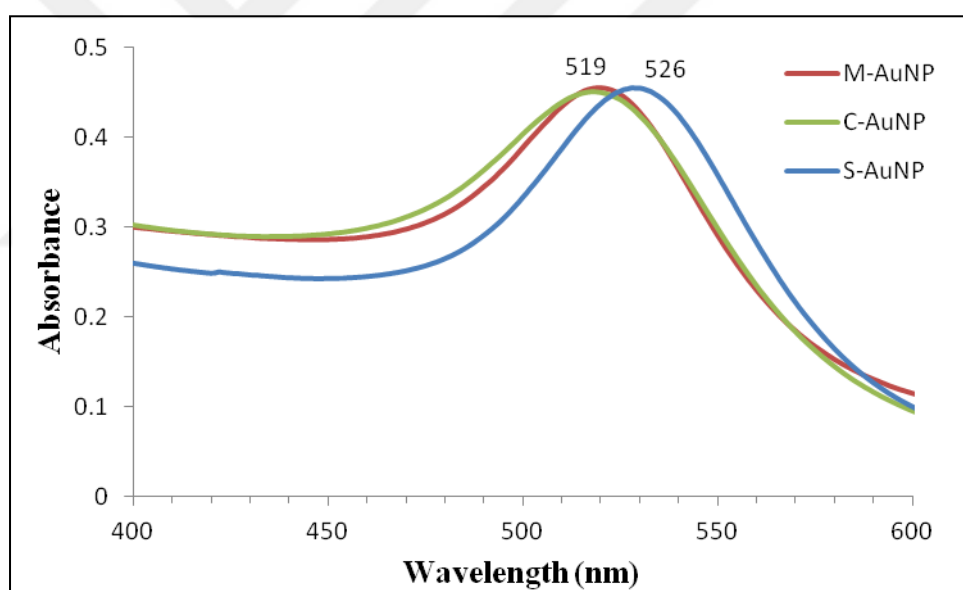


Figure 3.1. UV/Vis spectra of M-AuNPs, C-AuNPs and S-AuNPs.

The DLS measurement provides information about hydrodynamic sizes of M-AuNPs, C-AuNPs and S-AuNPs in aqueous environment. The DLS spectra of M-AuNP, C-AuNP and S-AuNP showed that they had 90, 16 and 60 nm hydrodynamic sizes, respectively as seen in Figure 3.2.

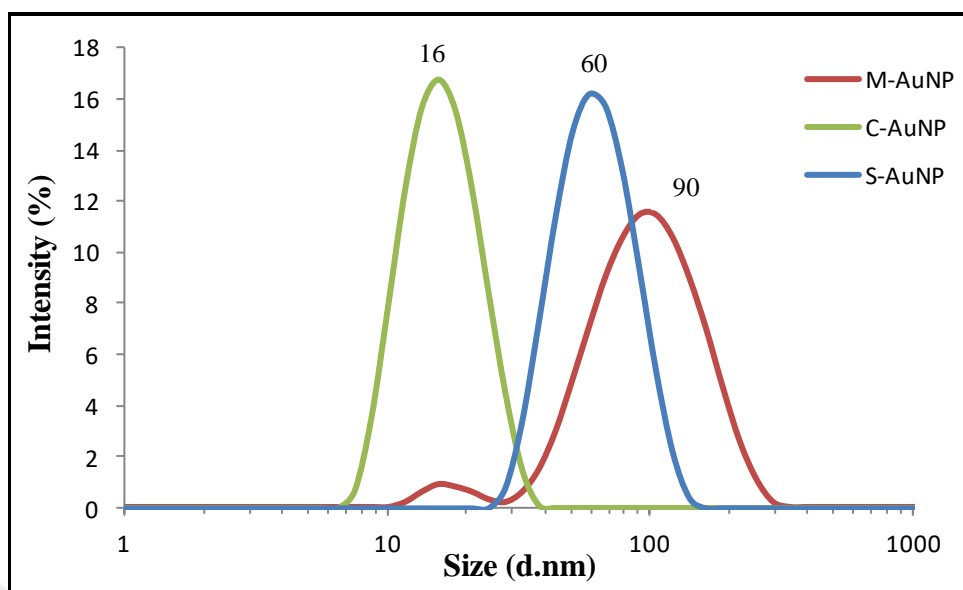


Figure 3.2. Size distribution of M-AuNP, C-AuNP and S-AuNP in DLS Analysis.

M-AuNPs were also examined on Atomic Force Microscopy (AFM). The size of M-AuNPs was measured as 12 nm approximately as seen in Figure 3.3 on line measurement.

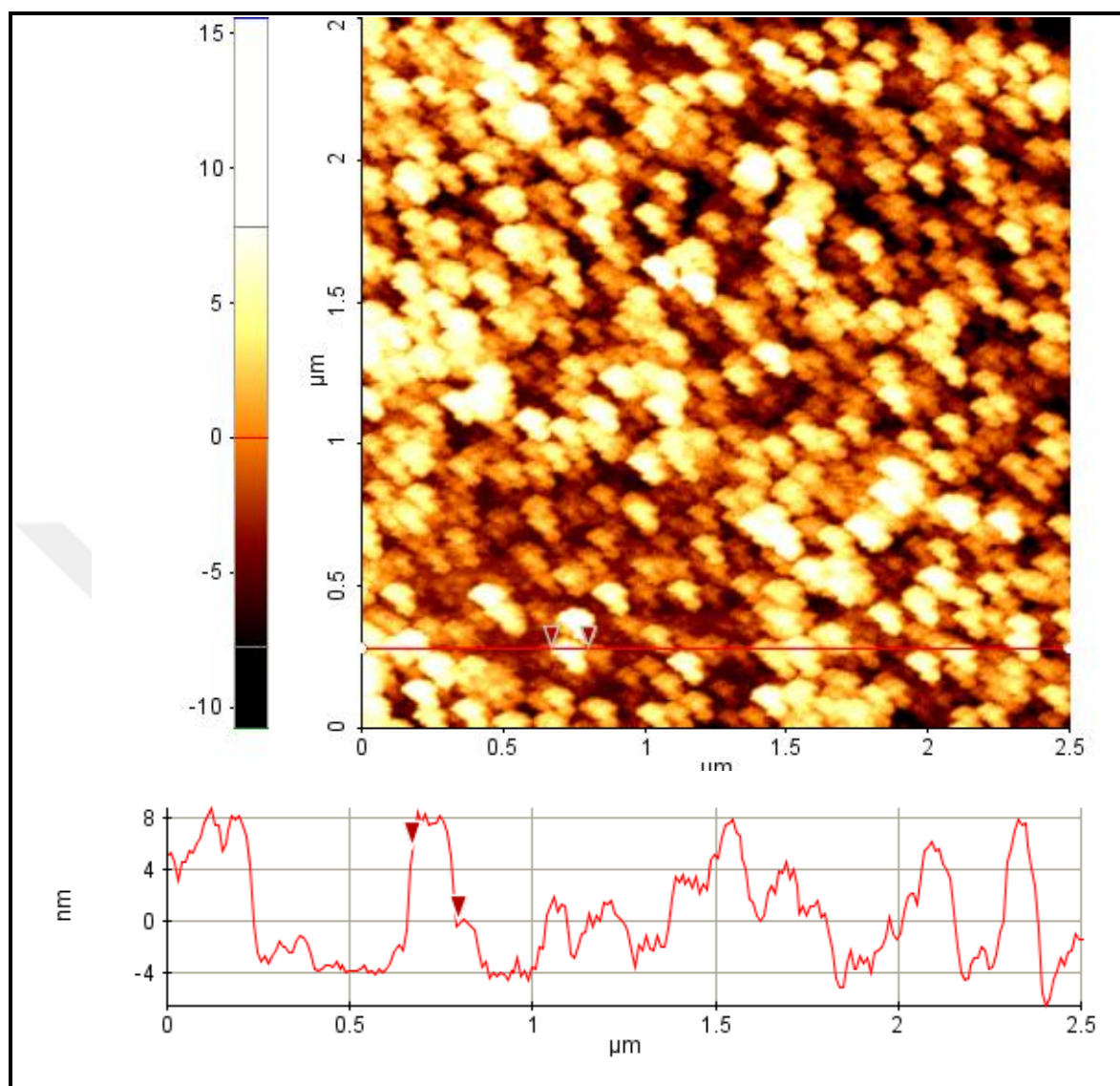


Figure 3.3. AFM image of M-AuNPs.

The images of bare and Dox conjugated M-AuNPs, C-AuNPs and S-AuNPs were shown in Figure 3.4. M-AuNPs and S-AuNPs were stable possessing similar color compared with their bare form, which may be an indication of high Dox-loading capacity while Dox addition to C-AuNPs changed the color of colloidal suspension to dark blue and caused precipitation of the particles immediately, which may be explained by lower stability and lower Dox loading capacity of C-AuNPs. A plausible explanation for the precipitations is due to the surface charge change of AuNPs as doxorubicin binds to the surface, which initiates aggregation.

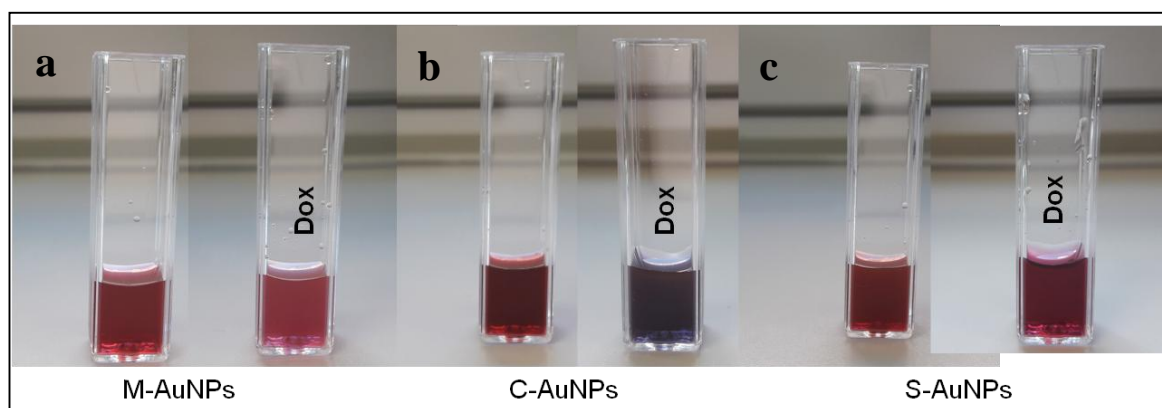


Figure 3.4. Image of (a) M-AuNPs, (b) C-AuNPs, (c) S-AuNPs and their Dox loaded forms.

The Dox-loaded M-AuNPs and S-AuNPs were characterized using UV/Vis absorption spectroscopy and DLS. After incubation of NPs with Dox for 24h, the solutions were centrifuged and free-Dox was removed from the solution. Final Dox concentration was calculated according to Dox absorbance spectrum which was about 2.5 μM Dox in final AuNP solutions. In Figure 3.5. and 3.6., the spectra of bare and Dox-conjugated M-AuNPs and S-AuNPs are shown respectively. A small redshift from 519 nm to 523 nm and a broadening of the absorption band were observed after Dox-loading of M-AuNPs as seen in Figure 3.5.

When S-AuNPs were conjugated to Dox, 2 nm redshift from 526 nm and broadening of the absorption peak were observed indicating that the Dox loading caused the agglomeration of the S-AuNPs as shown in Figure 3.6.

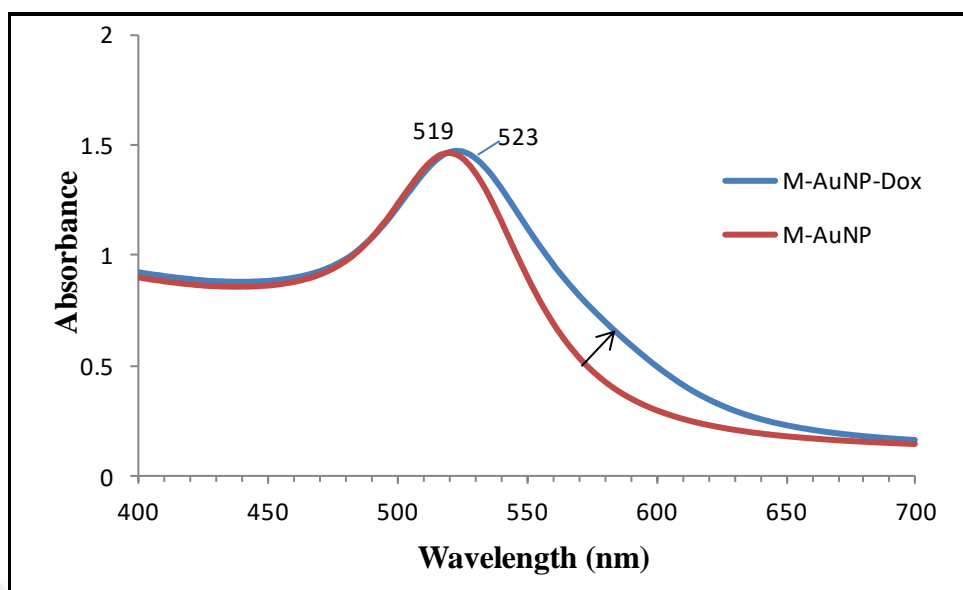


Figure 3.5. Comparison of absorption spectra of bare M-AuNPs and Dox-conjugated M-AuNPs.

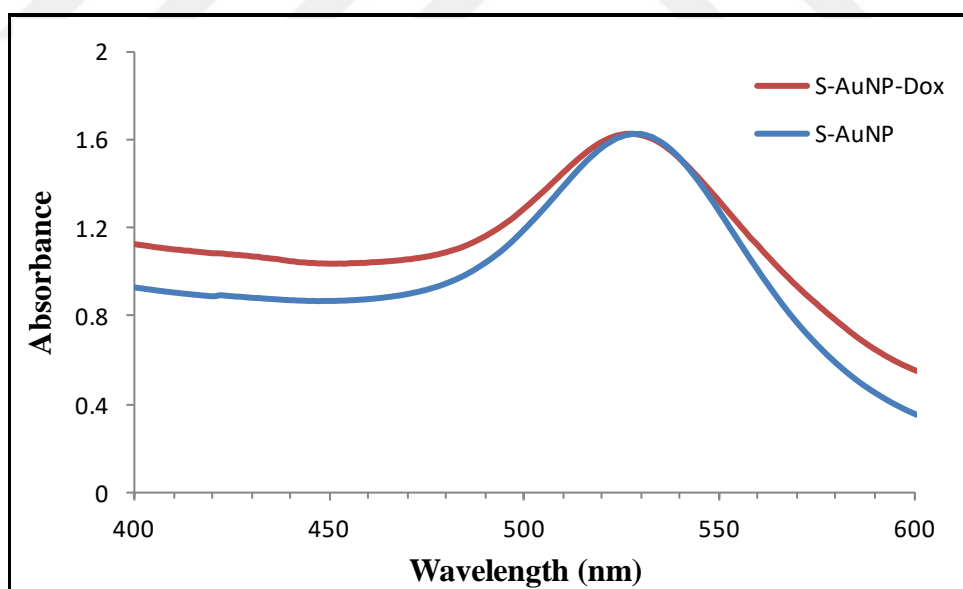


Figure 3.6. Comparison of absorption spectra of S-AuNP and Dox-conjugated S-AuNPs.

The reproducibility of the Dox loading of M-AuNPs was evaluated at different batches. As shown in Figure 3.7., AuNP-Dox conjugation reaction is reproducible which, the maximum absorbance wavelength of final solution is acquired at 522 nm.

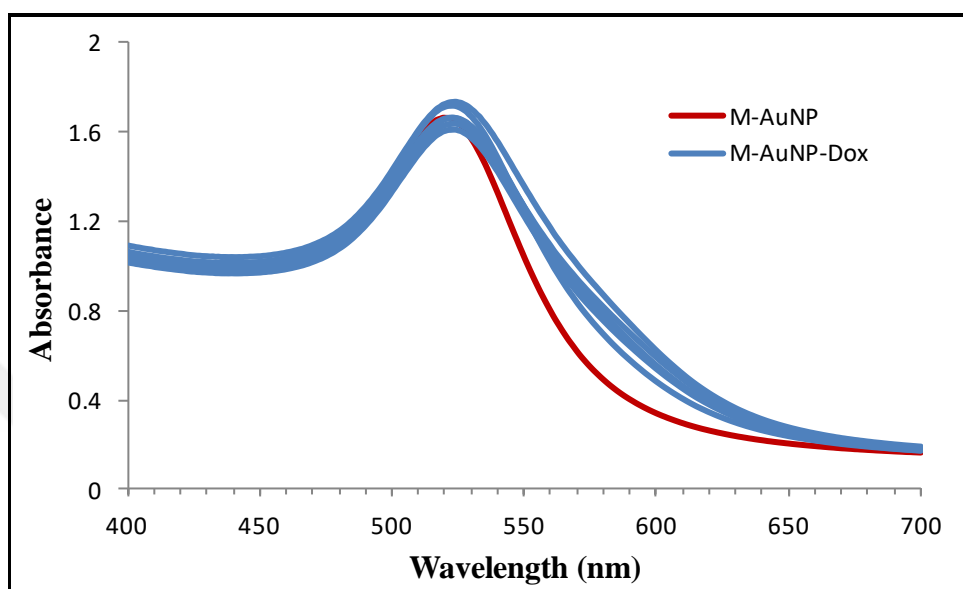


Figure 3.7. Reproducibility of AuNPs conjugation with Doxorubicin.

DLS spectra of Dox-loaded M-AuNPs and S-AuNPs were shown in comparison to their bare form in Figure 3.8. and Figure 3.9. The increase in hydrodynamic size also demonstrates the Dox loading on AuNPs. The final size of M-AuNPs and S-AuNPs were around 90-100 nm and 100-110 nm, respectively. While there was a small size change in M-AuNP-Dox, the size of S-AuNPs was doubled after loaded with Dox. This can be explained by the agglomeration of S-AuNPs after centrifugation and dispersion in dH₂O.

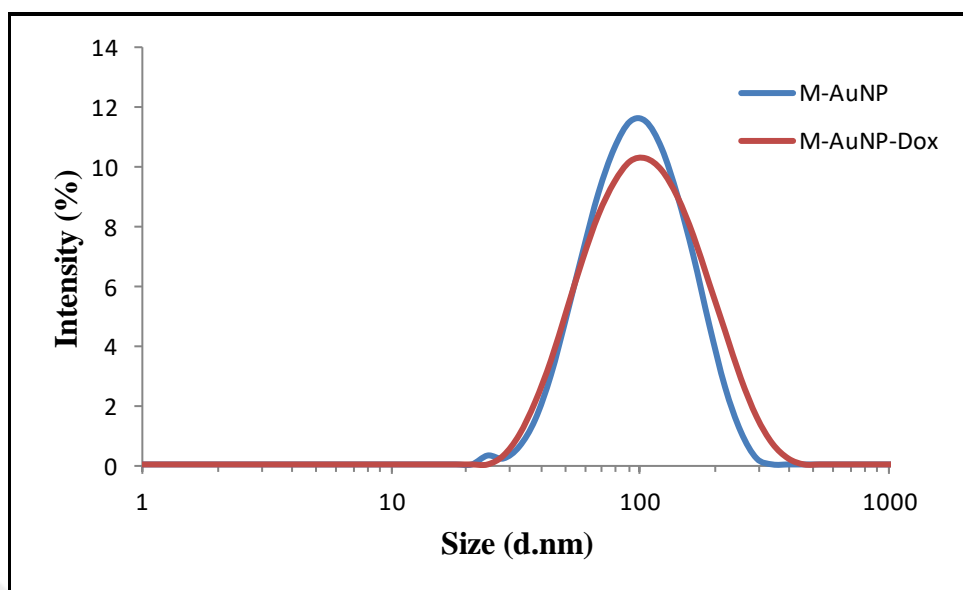


Figure 3.8. DLS spectra of bare and Dox-loaded M-AuNPs.

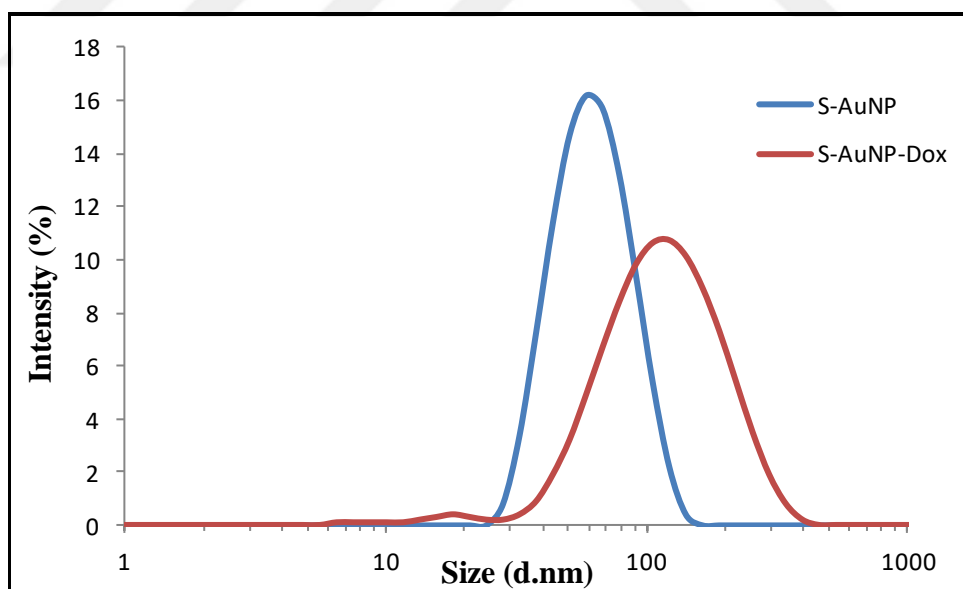


Figure 3.9. DLS spectra of bare and Dox-loaded S-AuNPs.

3.2. WST-1 CELL VIABILITY ASSAY

The influence of M-AuNPs, mannan, Dox-loaded M-AuNPs and Dox on PNT1A and DU145 cells was evaluated by measuring the mitochondrial activity. Cells were exposed to M-AuNPs at 0.35, 0.70 and 1.40 nM concentration. The concentration of free-mannan was selected in the 4.5, 9.0 and 18.0 $\mu\text{g/mL}$ range which is the amount of mannan used during the synthesis in the M-AuNPs. The Dox conjugated M-AuNPs (M-AuNPs-Dox) and free Dox exposure at 0.25, 0.5 and 1 μM concentrations were also compared in order to evaluate the efficiency of M-AuNPs on drug delivery for prostate cancer. The cell viability after exposure to mannan, M-AuNPs and M-AuNP-Dox was shown in Figure 3.10.

M-AuNPs and free-mannan did not show any cytotoxic effect on both PNT1A and DU145 cells. In PNT1A cells, cell viability is about 88% after M-AuNP-Dox treatment whereas free Dox treatment decreased the cell viability to 60% at 1 μM Dox concentration as seen in figure 3.10.B. The percent viability of Dox-loaded M-AuNPs treated DU145 cells was 61% whereas Dox treatment decreased the viability to 51% at 1 μM concentration.

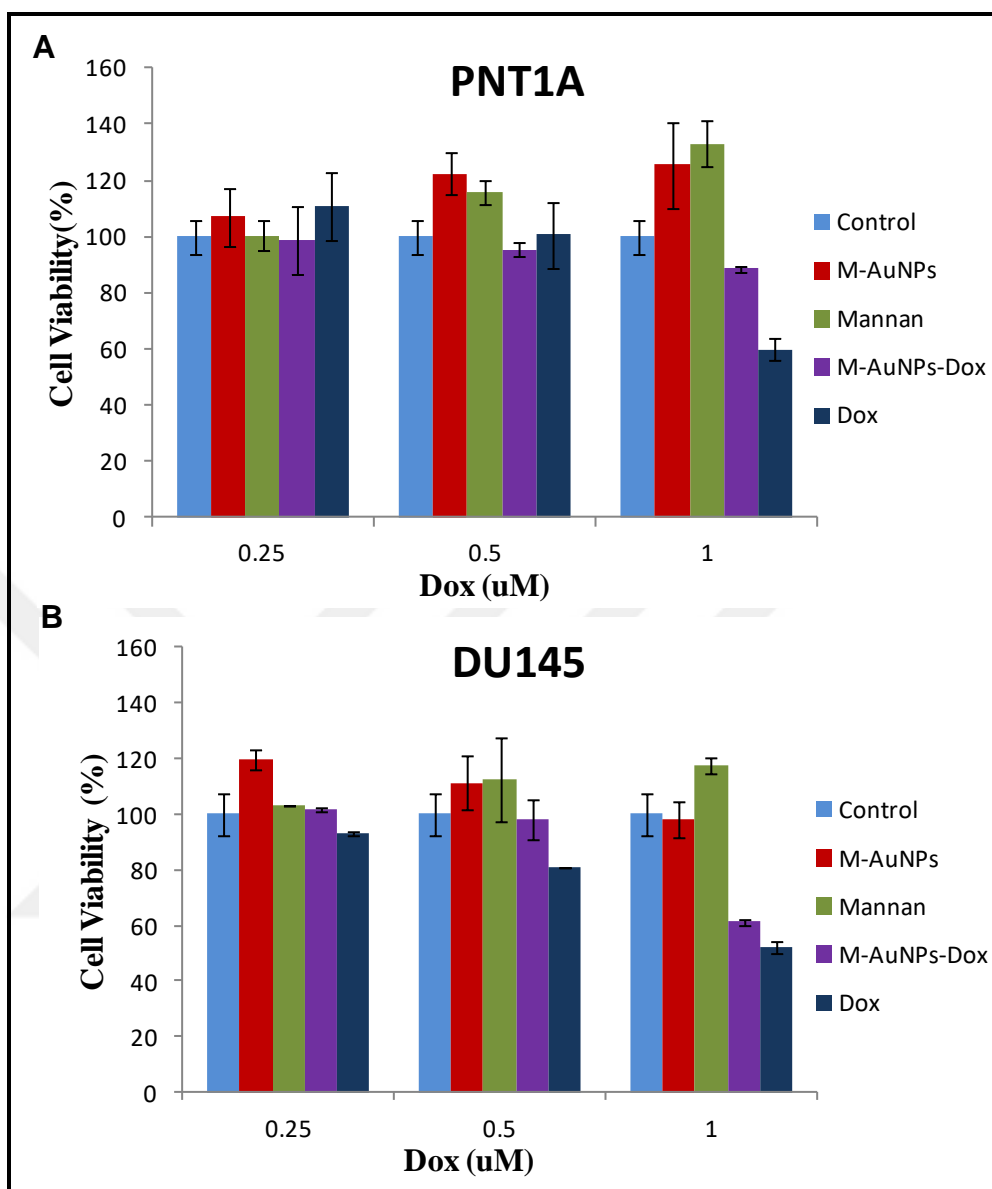


Figure 3.10. Cell viability of (A) PNT1A and (B) DU145 cells after exposure of M-AuNPs, free-mannan, M-AuNP-Dox and free-Dox for 24 h.

Since C-AuNPs could not be conjugated with Dox, it was not possible to make comparison between Dox-loaded C-AuNPs. The cytotoxic effect of bare C-AuNPs and M-AuNPs on PNT1A and DU145 cells were compared in Figure 3.11. Both C-AuNPs and M-AuNPs were observed not to be toxic for PNT1A and DU145 cells. C-AuNPs have increased the cell viability more than M-AuNPs.

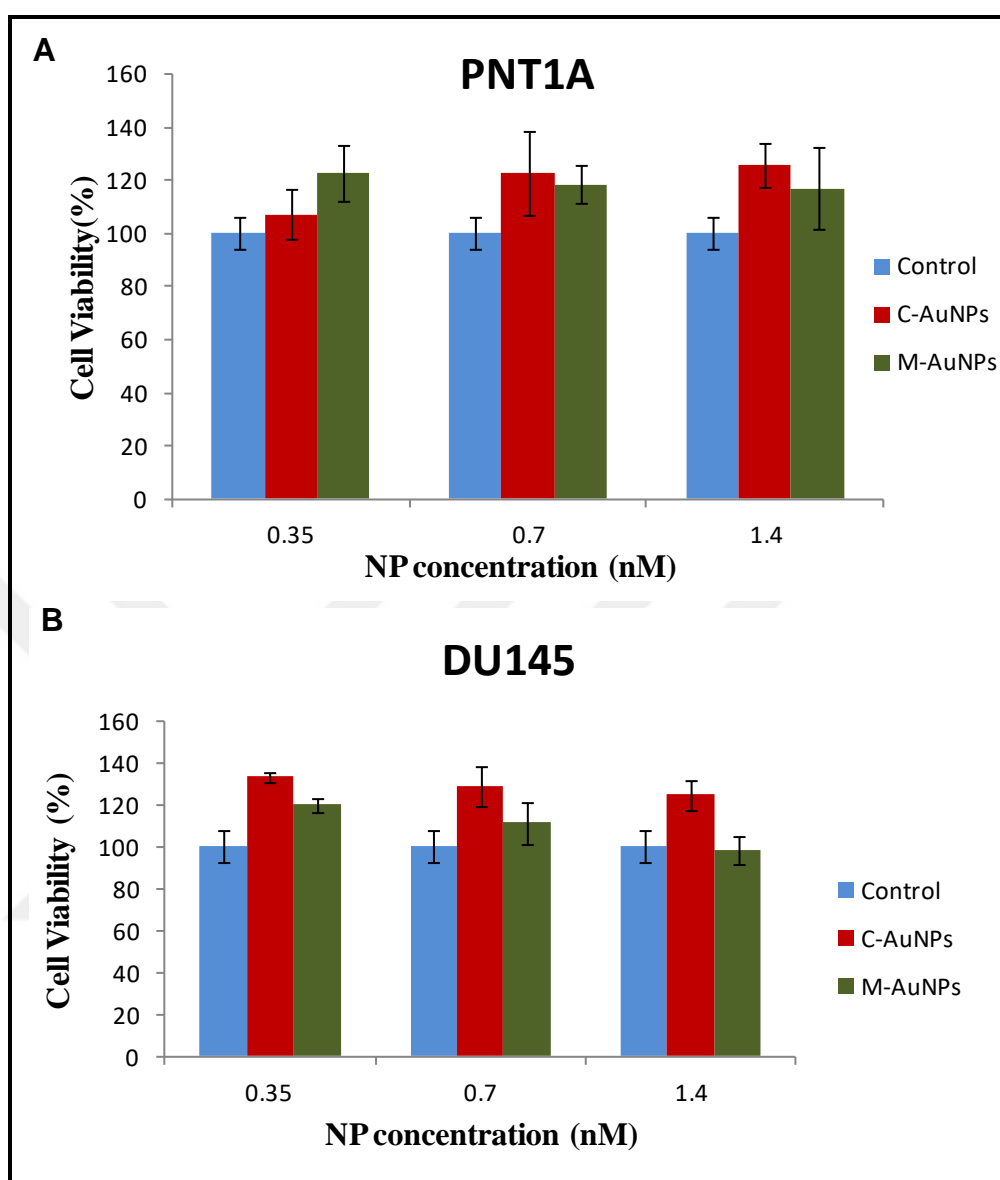


Figure 3.11. Cell viability of (A) PNT1A and (B) DU145 cells after exposure of M-AuNPs and C-AuNPs.

Starch as another polysaccharide, was used for reduction of AuNPs to show which polysaccharide would be more suitable for this drug delivery system. As shown in Figure 3.12, S-AuNPs did not show toxic effect on both PNT1A and DU145 cells in used concentration range. S-AuNP-Dox also showed cytotoxic effect on both PNT1A and DU145 cells after 1 μ M concentration of Dox. However, free-Dox treatment decreased the viability 5-10 % more at 1 μ M concentration on both cell lines.

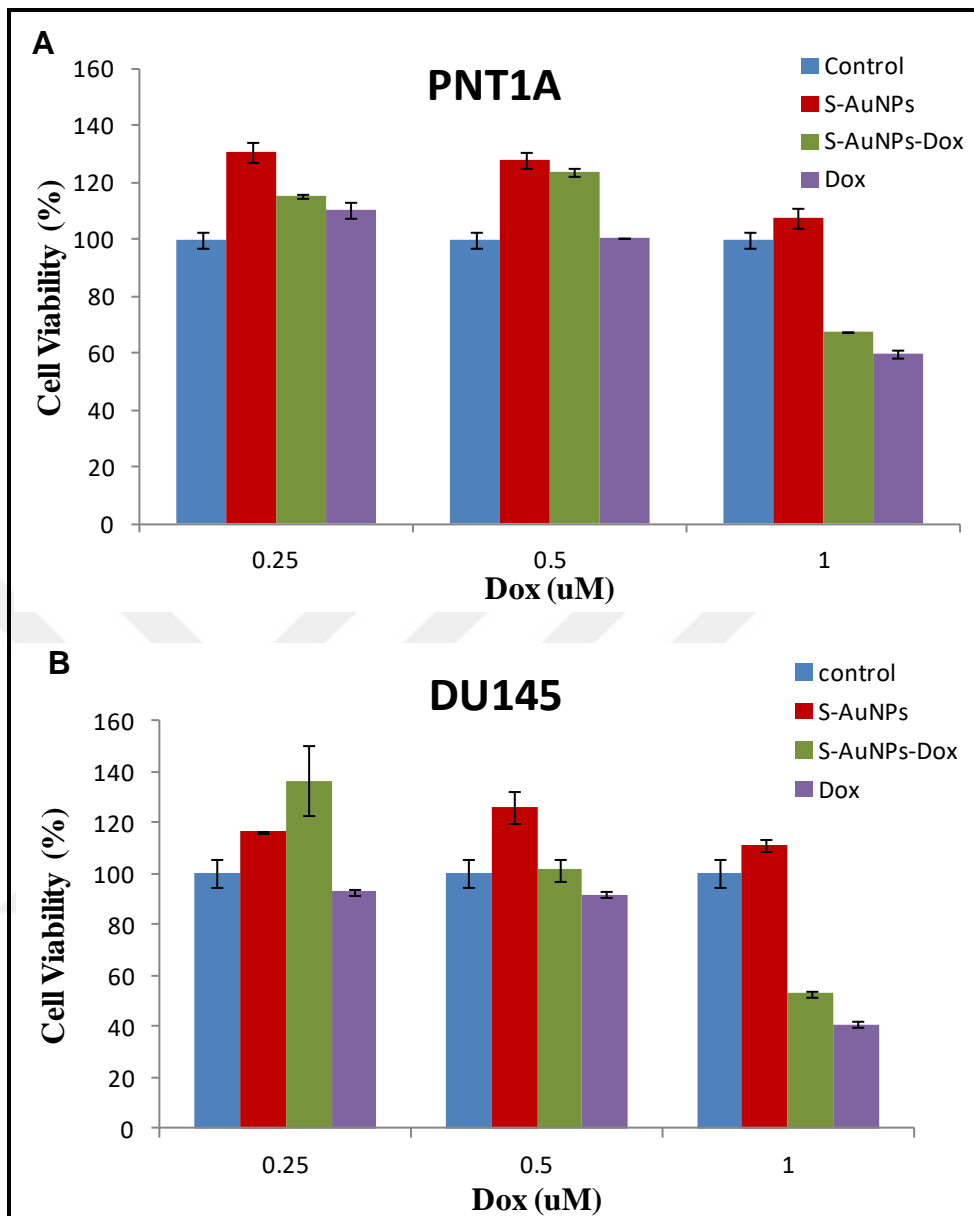


Figure 3.12. Cell viability of (A) PNT1A and (B) DU145 cells after exposure of S-AuNPs, free-Dox, and S-AuNP-Dox conjugates.

3.3. CELL CYCLE ANALYSIS

After penetration into nucleus, Dox blocks Topoisomerase-II enzyme and induces arrest in G₂/M phase [71]. However, there was an obvious effect of mannan-reduced AuNP on prostate cancer cells. The effects on the cell cycle and growth, were evaluated after treatment with Dox (0.5 μM), colchicine (0.1 μM), M-AuNP (3 nM) and Dox-AuNP conjugates (1 μM Dox loaded in 3 nM M-AuNP). Colchicine is a chemotherapeutic drug which causes cell cycle arrest in G₂/M phase as Dox does and it was used as positive control in the cell cycle studies.

In Table 3.1. and 3.2., the percentage of every cell cycle phases is shown and where the most of the cells are currently in PNT1A and DU145 cell lines, respectively.

In PNT1A healthy prostate cell, while colchicine and Dox causes cell arrest in G₂/M phase and M-AuNP shows the same cell cycle pattern as in untreated cell lines. Almost 75% of PNT1A cells treated with Dox-loaded M-AuNPs were in G₀/G₁ phase on the contrary of cells treated with only Dox.

Table 3.1. Cell cycle results of PNT1A cell line treated with Colchicine, M-AuNP, free-Dox and M-AuNP-Dox.

PNT1A	G₀/G₁ (%)	S (%)	G₂/M (%)
(-) Ctrl (Untreated)	45.14	21.08	32.17
(+)Ctrl (Colchicine)	12.53	11.37	74.9
M-AuNP	41.95	22.56	34.03
Dox	8.28	23.4	63.81
M-AuNP-Dox	74.52	9.18	17.16

In DU145 cells, however, compared to PNT1A cells, Dox-treated cells were not that much effective in DU145 cells, only one third of cells were in G₂/M, but Dox-loaded M-AuNPs caused higher arrest than others in G₂/M phase.

Table 3.2. Cell Cycle results of DU145 cell line treated with Colchicine, M-AuNP, free-Dox and M-AuNP-Dox.

DU145	G₀/G₁ (%)	S (%)	G₂/M (%)
(-) Ctrl (Untreated)	48.81	13.82	37.37
(+)Ctrl (Colchicine)	15.97	12.24	71.79
M-AuNP	48.38	17.94	33.69
Dox	33.8	34.29	31.91
M-AuNP-Dox	8.15	22.29	69.57

3.4. INTRACELLULAR ACCUMULATION OF M-AUNPs

The uptake efficiency of M-AuNPs by the prostate cancer cells was demonstrated by the accumulated amount of Au⁺² inside cells using ICP-MS. As shown in Table 3.3., M-AuNPs are accumulated inside DU145 cells almost twice than in PNT1A cells. Whilst there was 197.97 ng/mL of Au⁺² present in PNT1A cells, 360.41 ng/mL Au⁺² was found in DU145 cells.

Table 3.3. Amount of Au⁺² accumulated inside cells determined by ICP-MS.

	Amount of Au⁺² in PNT1A (ng/mL)	Amount of Au⁺² in DU145 (ng/mL)
(-) Negative Ctrl	17.63444 ± 12.40	0.52667 ± 1.59
M-AuNPs	197.9778 ± 31.79	360.416 ± 56.11

4. DISCUSSION

The rational design of nanocarrier systems for drug delivery applications plays important role to delivery of the cargo efficiently to the targeted area. The NPs have been modified with different biomolecules for targeted drug delivery systems to have more efficient transport and reduce cytotoxicity. Antibodies, aptamers, peptides, sugars or drugs can be conjugated on the surface of AuNPs [41]. Polysaccharide-modified nanocarrier systems can be used for targeting of carbohydrate recognizing receptors such as lectin. Especially in prostate cancer cells, it was shown that mannose-6-phosphate receptors, which are one type of lectins are over-expressed, but not in prostate and breast healthy cells [67]. When mannose residues are recognized by lectins, they are phagocytosed inside the cell [68]. However, most of procedures used for conjugation of biomolecules on the surface of AuNPs consist of linker or acidic chemicals, which can induce cytotoxicity after hydrolysis of NPs inside cells. For avoiding any unpredictable toxic effect of NPs in long term, in the synthesis procedure of AuNPs, no linker was used and AuNPs were synthesized with biomolecules directly.

In this purpose, mannan reduced gold nanoparticles were synthesized in order to use in targeted drug delivery for prostate cancer cells. In order to demonstrate the efficiency, the AuNPs were synthesized with three different reducing agents which are mannan, citrate and starch. By the virtue of that mannan is a polymer of mannose residues, mannan was chosen as reducing agent for targeted drug delivery to prostate cancer cells and investigated as a possible method for the treatment of prostate cancer. C-AuNPs and S-AuNPs were chosen to be compared with M-AuNPs in terms of efficiency and cytotoxicity because reduction by citrate method of AuNPs have been used widely in many biological applications and starch is very common carbohydrate which is also used for modification of NPs. The NPs were compared in terms of their SPR absorption, hydrodynamic size as well as cytotoxicity, cell uptake and effect on cell cycle on PNT1A and DU 145 cells. The synthesized AuNPs are in the range of 10-100 nm which clarifies the availability of these NPs for efficient drug delivery system due to the EPR effect, which the particles escape from physiological barriers more efficiently [42]. If nanoparticles are smaller than 10 nm, they are cleared from the body rapidly by kidneys or through the extravasation. If nanoparticle size is larger than 10 nm, they are more likely to be cleared from the body by

reticuloendothelial system [40]. According to DLS results, the size of M-AuNPs are greater than S-AuNPs, which has greater size than C-AuNPs.

The Dox loading capacities and stabilities of the M-AuNPs, C-AuNPs and S-AuNPs also showed differences. Since Dox is a positively charged molecule due to amine group on it and synthesized AuNPs are negatively charged, the conjugation reaction occurred non-covalently by electrostatic interactions. The M-AuNPs, C-AuNPs and S-AuNPs were mixed with Dox in the same concentration. The results showed that C-AuNPs aggregated immediately after the addition of Dox and the color of the solution turned to dark blue from red, while M-AuNPs and S-AuNPs had a color change to pink from red and had no aggregation. This results from the lower loading capacity and colloidal stability of C-AuNPs than in M-AuNPs and S-AuNPs.

The cytotoxic effect of C-AuNPs than in M-AuNPs and S-AuNPs on both healthy and cancerous prostate cells was evaluated and they were found not cytotoxic. The effect of Dox loaded AuNPs were also evaluated. Dox is commercially used as an anthracycline antibiotic [69]. It behaves in two ways in cancer cells. First one is that it generates free radicals and they damage DNA, cell membrane and proteins, so induces apoptotic cell death [70]. Second way is intercalating DNA. Dox penetrates into the cell, blocks Topoisomerase-II and causes arrest in G₂/M phase in cell cycle. This ends up with the cell death [71]. Dox has been used in treatment of many different types of cancer. Nevertheless, the main disadvantage of Dox is the lack of tumor targeting ability. Thus, it affects healthy cells beside cancerous cells [37]. Due to poor biodistribution, different strategies were developed to reduce side effects of Dox.

The influence of M-AuNPs, M-AuNP-Dox and Dox were compared to demonstrate the efficiency on prostate carcinoma cells by comparing prostate healthy cells. The influence of mannan was evaluated in order to discriminate the effect of NPs itself on the cells. Free-mannan and M-AuNPs did not show cytotoxic effect on both cell lines. After treatment of cells with 1 μ M Dox-loaded M-AuNP-Dox, the effect of Dox on the cells was observed by decreasing the cell viability to 60 %. When 1 μ M of free Dox is introduced to cells, in DU145 cells, free-Dox showed less viability around 51%. However, in PNT1A cells, it has been found that M-AuNP-Dox do not induce death as only Dox did, in which the cell viability was about 88% in healthy cells after treatment with M-AuNP-Dox whereas only 60% of PNT1A cells were alive after treatment with Dox. This result is promising because

it reveals that when Dox is loaded on M-AuNPs, it decreases the side effects of Dox on healthy cells but keeping efficient killing ability for cancerous cells.

S-AuNPs were also examined as a tool for treatment of prostate cancer. S-AuNP-Dox had decreased cell viability to 50% on DU145 cells while Dox reduced to 40 %. However, it also showed high toxic effect on PNT1A healthy cell lines so that cell viability was reduced to 70%. Thus, it can be interpreted as starch does not reduce side effects of Dox on healthy cell lines, as M-AuNP-Dox does.

To examine the effect of free-Dox and M-AuNP-Dox on prostate cells, cell cycle assays were performed. Similar to free-Dox treatment, M-AuNP-Dox showed cell arrest in G₂/M phase in cancerous cells whereas healthy cells were not arrested. On the contrary, cell growth was proceeding and most of the cells were in G₀/G₁ phase, indicating differential influence of M-AuNPs-Dox on healthy and cancerous cells.

For better interpretation of cytotoxicity and cell cycle results, intracellular accumulation of M-AuNPs was investigated. Almost double amount of M-AuNPs taken up into DU145 cancerous cells than in PNT1A healthy cells. This might be because of that prostate cancer cells have more lectin receptors which recognize mannose residues, on cell surface and this increases the uptake of NPs into cancerous cells than healthy cells.

5. CONCLUSIONS

In this study, M-AuNPs were synthesized to evaluate their possible use as drug delivery agent for prostate cancer treatment. Mannan is used to reduce to AuNPs with the aim of targeting the highly expressed mannose 6-phosphate receptor (M6PR) in prostate cancer cells. The selective uptake of M-AuNPs compared to S-AuNPs by prostate cancer cells was demonstrated. The results showed that the synthesized AuNPs did not influence the viability of the both cell lines. Dox-loaded AuNPs displayed a high rate of toxicity on DU145 cancer cells by inducing cell cycle arrest in G2/M phase. It was shown that the M-AuNPs could be used for transferring Dox in prostate cancer cells. The results indicate that M-AuNPs are more efficient nanocarrier than C-AuNPs and S-AuNPs for possible treatment of prostate cancer. In addition, once M-AuNPs carrying chemotherapy agent are accumulated in the tumor region, a NIR laser can be used to eliminate the tumor with thermal ablation since the aggregates of AuNPs strongly absorbs the light in the NIR region. Although access to prostate is invasive, a fiber optic with a less invasive procedure can be inserted to the ablation location. As alternative to intravenous injection of the prepared formulation, local injection can be considered to avoid the potential side effects of the prepared chemotherapy agent. Although further in vitro and in vivo studies are necessary to clarify the potential of M-AuNPs as multifunctional therapeutic agent, this study shows promising results for that direction.

REFERENCES

1. ASTM International. E 2456-06 Terminology for Nanobiotechnology. West Conshohocken, PA: ASTM International, 2006.
2. S.J. Douglas, S.S. Davis and L. Illum. Nanoparticles in Drug Delivery. *Critical Reviews in Therapeutic Drug Carrier Systems*, 3: 233-261, 1987.
3. K. Riehemann, S.W. Schneider, T.A. Luger, B. Godin, M. Ferrari and H. Fuchs. Nanomedicine—Challenge and Perspectives. *Angewandte Chemie International. Education*, 48: 872-897, 2009.
4. D.A. La Van, D.M. Lynn and R. Langer. Moving Smaller in Drug Discovery and Delivery. *Nature Reviews Drug Discovery*, 1:77-84, 2002.
5. R. Langer and D.A. Tirrell. Designing Materials for Biology and Medicine. *Nature*, 428: 487-92, 2004.
6. M.E. Lobatto, V. Fuster, Z.A. Fayad and W.J.M. Mulder. Perspectives and Opportunities for Nanomedicine in the Management of Atherosclerosis. *Nature Reviews Drug Discovery*, 10: 835-52, 2011.
7. G.A. Silva. Neuroscience Nanotechnology; Progress, Opportunities and Challenges. *Nature Reviews Neuroscience*, 7: 65-74, 2006.
8. O.S. Muddineti, B. Ghosh and S. Biswas. Current Trends in Using Polymer Coated Gold Nanoparticles for Cancer Therapy. *International Journal of Pharmaceutics*, 484: 252-267, 2015.
9. M.E. Davis, Z. Chen and D.M. Shin. Nanoparticle Therapeutics: An Emerging Treatment Modality for Cancer. *Nature Reviews Drug Discovery*, 7: 771-782, 2008.

10. N.T. Huynh, C. Passirani, P. Saulnier and J.P. Benoit. Lipid Nanocapsules: A New Platform for Nanomedicine. *International Journal of Pharmaceutics*, 379: 201-209, 2009.
11. C.C. Lee, J.A. MacKay, J.M.J. Frechet and F.C. Szoka. Designing Dendrimers for Biological Applications. *Nature Biotechnology*, 23: 1517-1526, 2005.
12. D. Peer, J.M. Karp, S. Hong, O.C. FaroKhazad, R. Margalit and R. Langer. Nanocarriers as An Emerging Platform for Cancer Therapy. *Nature Nanotechnology*, 2: 751-760, 2007.
13. V.P. Torchilin. Recent advances with liposomes as Pharmaceutical Carriers. *Nature Reviews Drug Discovery*, 4: 145-160, 2005.
14. S. Luo, J. Xu, Y. Zhang, S. Liu and C. Wu. Double Hydrophilic Block Copolymer Monolayer Protected Hybrid Gold Nanoparticles and Their Shell Cross-linking. *Journal of Physical Chemistry B*, 109: 22159-66, 2005.
15. X. Li, M. Takashima, E. Yuba, A. Harada and K. Kono. PEGylated PAMAM Dendrimer-Doxorubicin Conjugate-Hybridized Gold Nanorod for Combined Photothermal-Chemotherapy. *Biomaterials*, 35: 6576-6584, 2014.
16. E.E. Connor, J. Mwamuka, A. Gole, C.J. Murphy and M.D. Wyatt. Gold Nanoparticles are Taken Up by Human Cells but Do Not Cause Acute Cytotoxicity. *Small*, 1: 325-327, 2005.
17. M.E. Stewart, C.R. Anderton, L.B. Thomson, J. Maria, S.K. Gray, J.A. Rogers and R.G. Nuzzo. Nanostructured Plasmonic Sensors. *Chemical Reviews*, 108: 494-521, 2008.
18. K.P. Jain, X. Huang and I.H. El-Sayed. Review of Some Interesting Surface Plasmon Resonance-Enhanced Properties of Noble Metal Nanoparticles and Their Applications to Biosystems. *Plasmonics*, 2: 107-118, 2007.

19. Y.S. Jung, J. Wuenschell, H.K. Kim, P.Kaur and D.H. Waldeck. Blue-Shift of Surface Plasmon Resonance in A Metal Nanoslit Array Structure. *Optics Express*, 17: 16081-16092, 2009.
20. J.C. Love, L.A. Estroff, J.K. Kriebel, R.G. Nuzzo and G.M. Whitesides. Self-Assembled Monolayers of Thiolates on Metals as A Form of Nanotechnology. *Chemical Reviews*, 105: 1103-1169, 2005.
21. P. Ghosh, G. Han, M. De, C.K. Kim and V.M. Rotello. Gold Nanoparticles in Delivery Applications. *Advanced Drug Delivery Reviews*, 60: 1307-1315, 2008.
22. C.K. Kim, P. Ghosh and V.M. Rotello. Multimodal Drug Delivery Using Gold Nanoparticles. *Nanoscale*, 1: 61-67, 2009.
23. X.H. Gao, Y.Y. Ciu, R.M. Levenson, L.W.K. Chung and S.M. Nie. In Vivo Cancer Targeting and Imaging with Semiconductor Quantum Dots. *Nature Biotechnology*. 22: 969-976, 2004.
24. S. Rana, A. Bajaj, R. Mout and V.M. Rotello. Monolayer Coated Gold Nanoparticles for Delivery Applications. *Advanced Drug Delivery Reviews*, 64: 200-216, 2012.
25. A.B. Mariotto, K.R. Yabroff, Y. Shao, E.J. Feuer and M.L. Brown. Projections of the Cost of Cancer Care in the United States: 2010-2020. *Journal of National Cancer Institute*, 103: 117-128, 2011.
26. R.L. Siegel, K.D. Miller and A. Jemal. Cancer Statistics, 2015. *CA Cancer Journal for Clinicians*, 65: 5-29, 2015.
27. D.L. Suzman and E.S. Antonarakis. Castration-Resistant Prostate Cancer: Latest Evidence and Therapeutic Implications. *Therapeutic Advances in Medical Oncology*, 6: 167-19, 2014.

28. A.J. Chang, K.A. Autio, M. Roach 3rd and H.I. Scher. High-Risk Prostate Cancer-Classification and Therapy. *Nature Reviews Clinical Oncology*, 11: 308-323, 2014.
29. C.H. Heldin, K. Rubin, K. Pietras and A. Ostman. High Interstitial Fluid Pressure – An Obstacle In Cancer Therapy. *Nature Reviews Cancer*, 4: 806-813, 2004.
30. R.K. Jain. Transport of Molecules in the Tumor Interstitium: A Review. *Cancer Research*, 47: 3039-3051, 1987.
31. M.E. Davis, Z.G. Chen and D.M. Shin. Nanoparticle Therapeutics: An Emerging Treatment Modality for Cancer. *Nature Reviews Drug Discovery*, 7: 771-782, 2008.
32. I. Kola and J. Landis. Can the Pharamceutical Industry Reduce Attrition Rates? *Nature Reviews Drug Discovery*, 3: 711-716, 2004.
33. M.T. Morgan, Y. Nakanishi, D.J. Kroll, A.P. Griset, M.A. Carnahan, M. Wathier, N.H. Oberlies, G. Manikumar, M.C. Wani and M.W. Grinstaff. Dendrimer-Encapsulated Camptothecins: Increased Solubility, Cellular Uptake, and Cellular Retention Affords Enhanced Anticancer Activity In Vitro. *Cancer Research*, 66: 11913-11921, 2006.
34. J.W. Nichols and Y.H. Bae. EPR : Evidence and Fallacy. *Journal of Controlled Release*, 190: 451-464, 2014.
35. C. Eliasson, A. Loren, K.V:G.K. Murty, M. Josefson, M. Kall, J. Abrahamsson and K. Abrahamsson. Multivariate Evaluation of Doxorubicin Surface Enhanced Raman Spectra. *Spectrochimica Acta Part A*, 57: 1907-1915, 2001.
36. A.Z. Mirza and H. Shamshad. Preparation and Characterization of Doxorubicin Functionalized Gold Nanoparticles. *European Journal of Medicinal Chemistry*, 46: 1857-1860, 2011.

37. S. Aryal, J.J. Grailer, S. Pilla, D.A. Steeber and S. Gong. Doxorubicin Conjugated Gold Nanoparticles as Water-Soluble and pH-Responsive Anticancer Drug Nanocarriers. *Journal of Material Chemistry.*, 19: 7879-7884, 2009.
38. S. Dhar, E.M. Reddy, A. Shiras, V. Pokharkar and B.L.V. Prasad. Natural Gum Reduced/Stabilized Gold Nanoparticles for Drug Delivery Formulations. *Chemistry- A European Journal*, 14: 10244-10250, 2008.
39. M. Prabakaran, J.J. Grailer, S. Pilla, D.A. Steeber and S. Gong. Gold Nanoparticles with A Monolayer of Doxorubicin-Conjugated Amphiphilic Block Copolymer for Tumor Targeted Drug Delivery. *Biomaterials*, 30: 6065-6075, 2009.
40. R.A. Petros and J.M. DeSimone. Strategies in the Design of Nanoparticles for Therapeutic Applications. *Nature Reviews Drug Discovery*, 9: 615-627, 2010.
41. A. Swami, J. Shi, S. Gadde, A.R. Votruba, N. Kolishetti and O.C. Farokhzad. Nanoparticles for Targeted and Temporally Controlled Drug Delivery. In: S. Svenson and R.K. Prud'homme, editors, *Multifunctional Nanoparticles for Drug Delivery Applications: Imaging, Targeting and Delivery*, Nanostructure Science and Technology, Springer Science+ Business Media, 2012.
42. F. Alexis, E. Pridgen, L.K. Molnar and O.C. Farokhzad. Factors Affecting the Clearance and Biodistribution of Polymeric Nanoparticles. *Molecular Pharmaceutics*, 5: 505-515, 2008.
43. M. Roser, D. Fischer and T. Kissel. Surface-Modified Biodegradable Albumin Nano- and Microspheres. II: Effect of Surface Charges on In Vitro Phagocytosis and Biodistribution in Rats. *European Journal of Pharmaceutics and Biopharmaceutics*, 46: 255-263, 1998.
44. R.A. Schwendener, P.A. Lagocki and Y.E. Rahman. The Effects of Charge and Size on the Interaction of Unilamellar Liposomes with Macrophages. *Biochimica et Biophysica Acta (BBA) – Biomembranes*, 772: 93-101, 1984.

45. C. Salvador-Morales, L. Zhang, R. Langer and O.C. Farokhzad. Immunocompatibility Properties of Lipid-Polymer Hybrid Nanoparticles with Heterogeneous Surface Functional Groups. *Biomaterials*, 30: 2231-2240, 2009.
46. M.E. Davis. The First Targeted Delivery of siRNA in Humans via A Self-Assembling Cyclodextrin Polymer-based Nanoparticle: from Concept to Clinic. *Molecular Pharmaceutics*, 6: 659-668, 2009.
47. P.S. Chauhan, N. Puri, P. Sharma and N. Gupta. Mannanases: Microbial sources, Production, Properties and Potential Biotechnological Applications. *Applied Microbiology and Biotechnology*, 93: 1817-1830, 2012.
48. K.S. Mikkonen and M. Tenkanen. Sustainable Food-Packaging Materials Based on Future Biorefinery Products: Xylans and Mannans. *Trends in Food Science and Technology*, 28: 90-102, 2012.
49. L.R.S. Moreira and E.X.F. Filho. An Overview of Mannan Structure and Mannan Degrading Enzyme Systems. *Applied Microbiology and Biotechnology*, 79: 165-178, 2008.
50. P. Pienpinijtham, X.X. Han, S. Ekgasit and Y. Ozaki. Highly Sensitive and Selective Determination of Iodide and Thiocyanate Concentrations Using Surface-Enhanced Raman Scattering of Starch-Reduced Gold Nanoparticles. *Journal of Analytical Chemistry*, 83:3655-3662, 2011.
51. D.A. Handley. In: N.A. Hayat (editor). *Colloidal Gold: Principles, Methods and Applications*. Academic Press, 1989.
52. X. Huang and M.A. El-Sayed. Gold Nanoparticles: Optical Properties and Implementations in Cancer Diagnosis and Photothermal Therapy. *Journal of Advanced Research*, 1:13-28, 2010.
53. R.D. Issels, L.H. Lindner, J. Verweij, P. Wust, P. Reichardt and B.C. Schem. Neoadjuvant Chemotherapy Alone or with Regional Hyperthermia for Localized High-risk

Soft-tissue Sarcoma: A Randomised Phase 3 Multicentre Study. *The Lancet Oncology*, 11: 561-570, 2010.

54. J. van der Zee, D. Gonzales, G.C. van Rhoon, J.D.P. van Dijk, V.L.J. van Putten and A.A.M. Hart. Comparison of Radiotherapy Alone with Radiotherapy Plus Hyperthermia in Locally Advanced Pelvic Tumours: A Prospective, Randomised, Multicentre Trial. *The Lancet Oncology*, 355: 1119-1125, 2000.

55. C.C. Vernon, J.W. Hand, S.B. Field, D. Machin, J.B. Whaley and J. Van der Zee. Radiotherapy with or without Hyperthermia in the Treatment of Superficial Localized Breast Cancer: Results from Five Randomized Controlled Trials. *International Journal of Radiation Oncology Biology Physics*, 35: 731-744, 1996.

56. P. Wust, B. Hildebrandt, G. Sreenivasa, B. Rau, J. Gellermann and H. Riess. Hyperthermia in Combined Treatment of Cancer. *The Lancet Oncology*, 3: 487-497, 2002.

57. W. Zhang, X. Zheng, S. Shen and X. Wang. Doxorubicin-loaded Magnetic Nanoparticle Clusters for Chemo-photothermal Treatment of the Prostate Cancer Cell Line PC3. *Biochemical and Biophysical Research Communications*, 466: 278-282, 2015.

58. G. Tian, X. Zhang, X. Zheng, W. Yin, L. Ruan and X. Liu. Multifunctional Rbx WO₃ Nanorods for Simultaneous Combined Chemo-photothermal Therapy and Photoacoustic/CT Imaging. *Small*, 10:4160-4170, 2014

59. E. Ju, Z. Li, Z. Liu, J. Ren and X. Qu. Near-infrared Light-triggered Drug-delivery Vehicle for Mitochondria-targeted Chemo-photothermal Therapy. *ACS Applied Materials & Interfaces*, 6: 4364-4370, 2014.

60. P. Cherukuri and S.A. Curley. Use of Nanoparticles for Targeted, Noninvasive Thermal Destruction of Malignant Cells. *Methods in Molecular Biology*, 624: 359-373, 2010.

61. S. Jain, D.G. Hirst and J.M. O'Sullivan. Gold Nanoparticles as Novel Agents for Cancer Therapy. *The British Journal of Radiology*, 85: 101-113, 2012.
62. S. Uthaman, S.J. Lee, K. Cherukula, C. Cho and I. Park. Polysaccharide-coated Magnetic Nanoparticles for Imaging and Gene Therapy. *BioMed Research International*, 2015: 1-14, 2015.
63. D.H. Dube and C.R. Bertozzi. Glycans in Cancer and Inflammation – Potential for Therapeutics and Diagnostics. *Nature Reviews Drug Discovery*, 4:477-488, 2005.
64. S. Hakomori. Glycolysation Defining Cancer Malignancy: New Wine in an Old Bottle. *Proceedings of the National Academy of Sciences U.S.A*, 99: 10231-10233, 2002.
65. Y.J. Kim and A. Varki. Perspectives on the Significance of Altered Glycosylation of Glycoproteins in Cancer. *Glycoconjugate journal*, 14: 569-576, 1997.
66. B.D. Chithrani, A.A. Ghazani and W.C.W. Chan. Determining the Size and Shape Dependence of Gold Nanoparticle Uptake into Mammalian Cells. *Nano Letters*, 6:662-668, 2006.
67. O. Vaillant, K. El Cheikh, D. Warther, D. Brevet, M. Maynadier, E. Bouffard, F. Salgues, A. Jeanjean, P. Puche, C. Mazerolles, P. Maillard, O. Mongin, M. Blanchard-Desce, L. Raehm, X. Rebillard, J. Durand, M. Gary-Bobo, A. Morere and M. Garcia. Mannose-6-Phosphate Receptor: A Target for Theranostics of Prostate Cancer. *Angewandte Communications International Editions*, 54: 5952-5956, 2015.
68. A.I. Beat and A-L. Michel. Adhesion Mechanisms Regulating the Migration of Monocytes. *Nature Reviews of Immunology*, 4: 432-444, 2004.
69. F. Arcamone, G. Cassinelli, G. Fantini, A. Grein, P. Orezzi and C. Pol. Adriamycin, 14-hydroxydaunomycin: a New Antitumor Antibiotic from *S. Peuceetius* var. *Caesius*. *Biotechnology and Bioengineering*, 11:1101–1110, 1969.

70. J.H. Doroshow. Role of Hydrogen Peroxide and Hydroxyl Radical Formation in the Killing of Ehrlich Tumor Cells by Anticancer Quinones. *Proceedings of the National Academy of Sciences U.S.A*, 83:4514–4518, 1986.
71. K.M. Tewey, T.C. Rowe, L. Yang, B.D. Halligan and L.F. Liu. Adriamycin-induced DNA Damage Mediated by Mammalian DNA Topoisomerase-II. *Science*, 226:466–468, 1984.
72. A.E. Nel, L. Madler and D. Velegol. Understanding Biophysicochemical Interactions at the Nano-bio Interface. *Nature Materials*, 8: 543557, 2009.
73. S. Eustis and A. El-Sayed. Why Gold Nanoparticles are More Precious Than Pretty Gold: Noble Metal Surface Plasmon Resonance and Its Enhancement of the Radiative and Nonradiative Properties of Nanocrystals of Different Shapes. *Chemical Society Reviews*, 35: 209-217, 2006.
74. M.P. Pileni. Nanosized Particles Made in Colloidal Assemblies. *Langmuir*, 13: 3266-3276, 1997.
75. K. Okitsu, M. Ashokkumar and F. Grieser. Sonochemical Synthesis of Gold Nanoparticles: Effects of Ultrasound Frequency. *The Journal Physical Chemistry B*, 109: 20673-20675, 2005.
76. S.R. Hall, W. Shenton, H. Engelhardt and S. Mann. Site-Specific Organization of Gold Nanoparticles by Biomolecular Templating. *Chem Phys Chem*, 2: 141-191, 2001.
77. S. Sun, P. Mendes, K. Critchley, S. Diegoli, M. Hanwell, S.D. Evans, G.J. Leggett, J.A. Preece and T.H. Richardson. Fabrication of Gold Micro and Nanostructures by Photolithography Exposure of Thiol Stabilized Gold Nanoparticles. *Nano Letters*, 6: 345-350, 2006.

78. P.A. Schaal, A. Besmehn, E. Maynicke, M. Noyong, B. Beschoten and U. Simon. Electrically Conducting Nanopatterns Formed by Chemical e-Beam Lithography via Gold Nanoparticle Seeds. *Langmuir*, 28: 2448-2454, 2012.
79. J. Turkevich, P.C. Stevenson and J. Hillier. A Study of the Nucleation and Growth Process in the Synthesis of Colloidal Gold. *Discussions of the Faraday Society*, 11: 55-75, 1951.
80. M. Shah, V. Badwaik, Y. Kherde, H.K. Waghvani, T. Modi, Z. P. Aguilar, H. Rodgers, W. Hamilton, T. Marutharaj, C. Webb, M. B. Lawrenz and R. Dakshinamurthy. Gold Nanoparticles: Various Methods of Synthesis and Antibacterial Applications. *Frontiers in Bioscience*, 19: 1320-1344, 2014.
81. M. Brust, M. Walker, W. Bethell, D.J. Schrifin, R. Whyman. Synthesis of Thiol-derivatised Gold Nanoparticles in a Two Phase Liquid System. *Journal of Chemical Society*, 801-802, 1994.
82. X. Zhi-Chuan, S. Cheng-Min, X. Cong-Wen, Y. Tian-Zhong, Z. Huai-Ruo, L. Jian-Qi and G. Hong-Jun. Wet Chemical Synthesis of Gold Nanoparticles Using Silver Seeds: A Shape Control from Nanorods to Hollow Spherical Nanoparticles. *Nanotechnology*, 18: 115608, 2007.
83. C.J. Murphy, T.K. Sau, A.M. Gole, C.J. Orendorff, J. Gao, L. Gou, S.E. Hunyadi and T. Li. Anisotropic Metal Nanoparticles: Synthesis, Assembly, and Optical Applications. *Journal of Physical Chemistry B*, 109: 13857–13870, 2005.
84. P.T. Anastas and J.C. Warner: Green Chemistry: Theory and Practice. *Oxford University Press: New York*, 30, 1998.
85. V. Apostolopoulos, G.A. Pietersz, A. Tsibanis, A. Tsikkinis, H. Drakaki, B.E. Loveland, S. J. Piddleston, M. Plebanski, D. S. Pouniotis, M. N. Alexis, I.F. McKenzie and S. Vassilaros. Pilot Phase III Immunotherapy Study in Early-stage Breast Cancer Patients Using Oxidized Mannan-MUC1. *Breast Cancer Research*, 8 R27, 2006.

86. S.A. Ferreira, P. Pereira, P. Sampaio, P. J. G. Coutinho and F. M. Gama. Supramolecular Assembled Nanogel Made of Mannan. *Journal of Colloid Interface Science*, 361: 97, 2011.
87. S.A. Ferreira, V. Carvalho, C. Costa, J.P. Teixeira, M. Vilanova and F.M. Gama. Self-assembled Mannan Nanogel: Cytocompatibility and Cell Localization. *Journal of Biomedical Nanotechnology*, 8: 1-9, 2012.
88. H. Vu-Quang, M. Muthiah, Y.K. Kim, C.S. Cho, R. Namgung, W.J. Kim, J. H. Rhee, S.H. Kang, S. Y. Jun, Y. J. Choi, Y.Y. Jeong and I. K. Park. Carboxylic Mannan-coated Iron Oxide Nanoparticles Targeted to Immune Cells for Lymph Node-specific MRI *in vivo*. *Carbohydrate Polymers*, 88: 780-788, 2012.
89. M. Ancui, W. Chengjun, D. Yimin and G. Jianwei. Research on the Medicinal Polymer Material Konjac Glucomannan. *Journal of Dali University*, 2: 004, 2009.
90. A. Kaur, S. Jain and A. K. Tiwary. Mannan-coated Gelatin Nanoparticles for Sustained and Targeted Delivery of Didanosine: In vitro and In vivo Evaluation. *Acta Pharmaceutica*. 58: 61-74, 2008.
91. V-K. Lakshmanan. Therapeutic Efficacy of Nanomedicines for Prostate Cancer: An Update. *Investigate and Clinical Urology*, 57: 21-29, 2016.
92. N. Goodarzi, M.H. Ghahremani, M.Amini, F. Atyabi, S.N. Ostad and N. Shabani Ravari. CD44-targeted Docetaxel Conjugate for Cancer Cells and Cancer Stem-like Cells: A Novel Hyaluronic Acidbased Drug Delivery System. *Chemical Biology and Drug Design*, 83: 741-752, 2014.
93. C.J. Weng and G.C. Yen. Flavonoids, A Ubiquitous Dietary Phenolic Subclass, Exert Extensive in vitro Anti-invasive and in vivo Antimetastatic Activities. *Cancer Metastasis Reviews*, 31: 323-351, 2012.

94. A. Castro Nava, M. Cojoc, C. Peitzsch, G. Cirillo, I. Kurth and S. Fuessel. Development of Novel Radiochemotherapy Approaches Targeting Prostate Tumor Progenitor Cells Using Nanohybrids. *International Journal of Cancer*, 137: 2492-2503, 2015.
95. H. Kulhari, D. Pooja, S. Shrivastava, S.R. Telukutala, A.K. Barui and C.R. Patra CR. Cyclic-RGDfK Peptide Conjugated Succinoyl-TPGS Nanomicelles for Targeted Delivery of Docetaxel to Integrin Receptor Over-expressing Angiogenic Tumours. *Nanomedicine*, 11: 1511-1520, 2015.
96. M. Li, F. Lin, Y. Lin and W. Peng. Extracellular Polysaccharide from Bordetella Species Reduces High Glucose-induced Macrophage Apoptosis via Regulating Interaction Between Caveolin-1 and TLR4. *Biochemical and Biophysical Research Communications*, 466: 748-754, 2015.
97. S.M. Axiak-Bechtel, A. Upendran, J.C. Lattimer, J. Kelsey, C. S. Cutler and K.A. Selting. Gum Arabic-coated Radioactive Gold Nanoparticles Cause No Short-term Local or Systemic Toxicity in the Clinically Relevant Canine Model of Prostate Cancer. *International Journal of Nanomedicine*, 9: 5001-5011, 2014.